AuPS Meeting - Melbourne 2008

Lunch and Posters

Tuesday 2 December 2008 − Alan Gilbert Building

PGC-1α reduces proteasome and lysosome activity and attenuates myotube protein degradation

P. Sepulveda, M.J. Quick, M.A. Wallace, R.J. Snow and A.P. Russell, The Centre for Physical Activity and Nutrition Research (C-PAN), School of Exercise and Nutrition Sciences, Deakin University, VIC 3125, Australia.

Introduction. Skeletal muscle adapts to physiological demands by altering its metabolism and modifying its size (Schiaffino *et al.,* 2007). Regulation of muscle size is determined by two opposite phenomena, hypertrophy and atrophy. The ubiquitin proteasome pathway (UPP) is seen as the predominate pathway involved in muscle protein degradation (Solomon & Goldberg, 1996), however, recently the lysosomal pathway has been shown to play a key role in myotube protein degradation (Zhao *et al.,* 2007). Peroxisome Proliferator - activated receptor gamma, co-activator 1 alpha (PGC1α), a key protein involved in oxidative metabolism, has been shown to attenuate atrophy in mice, in part, *via* inhibiting the Forkhead (FoXO) transcriptional regulation of atrogin-1 and MuRF1 (Sandri *et al.,* 2006), two key members of the UPP (Bodine *et al.,* 2001). Whether PGC-1α influences proteasomal and lysosomal activity is unknown.

Methods. Mouse C2C12 myotubes were infected for 48 h with an adenovirus (Adv) containing green fluorescent protein (GFP-Adv) or human PGC-1α (hPGC-1α-Adv). After infection, myotubes were treated with or without dexamethasone (DEX) (10 μM) for 24 h and the release of [^{3}H]-tyrosine into the media was used as a measure of protein degradation. Proteasomal chymotrypsin- and caspase-like activities, as well as lysosomal cathepsin protease activity was measured *via* fluorometric analysis of their cleaved fluorescent peptide substrates, Suc-LLVY-AMC, Z-Leu-Leu-Glu-MCA and Z-Phe-Arg-AMC·HCl, respectively. Expression of PGC-1α, atrogin-1 and MuRF1 mRNA were measured *via* quantitative PCR.

Results. When compared to the GFP-Adv control group, over expressing hPGC-1α in C2C12 myotubes attenuated basal as well as DEX induced protein degradation by 18% and 33%, respectively. PGC-1α blunted proteasomal chymotrypsin- and caspase-like activities, and lysosomal cathepsin activity by 42%, 43% and 64%, respectively and reduced atrogin-1 and MuRF1 mRNA levels by 50% and 74%, respectively.

Conclusions. Our results demonstrate that PGC-1α attenuates both basal and DEX induced protein degradation, in part, *via* reducing the activities of the proteasome and lysosome. The reductions in atrogin-1 and MuRF1 support previous observations and suggest a possible mechanism influencing the reduced proteasomal activity. Further investigations are required to determine how PGC-1α attenuates proteasomal and lysosomal activity.

Bodine SC, Latres E, Baumhueter S, Lai VK, Nunez L, Clarke BA, Poueymirou WT, Panaro FJ, Na E, Dharmarajan K, Pan ZQ, Valenzuela DM, DeChiara TM, Stitt TN, Yancopoulos GD & Glass, DJ. (2001) *Science*, **294:** 1704-8.

Sandri M, Lin J, Handschin C, Yang W, Arany ZP, Lecker SH, Goldberg AL & Spiegelman BM. (2006) *Proceedings of the National Academy of Sciences USA*, **103:** 16260-5.

Schiaffino S, Sandri M & Murgia M. (2007) *Physiology (Bethesda)*, **22:** 269-78.

Solomon V & Goldberg AL. (1996). *Journal of Biological Chemistry* **271:** 26690-7.

Zhao J, Brault JJ, Schild A, Cao P, Sandri M, Schiaffino S, Lecker SH & Goldberg AL. (2007) *Cell Metabolism* **6:** 472-83.

Effect of mechanical stretching on Akt signalling and protein synthesis in myotubes

E.L. Brown, M.J. Quick, R.J. Snow and A.P. Russell, The Centre for Physical Activity and Nutrition Research (C-PAN), School of Exercise and Nutrition Sciences, Deakin University, VIC 3125, Australia.

Introduction. Recently, studies using pharmacological and genetic modifications in rodents and cells have found the protein kinase Akt (protein kinase B) to be a major regulator of muscle mass. When active, Akt increases protein synthesis *via* signalling through the mammalian target of rapamycin (mTOR) and glycogen synthase kinase-3β (GSK-3β), and inhibits protein degradation *via* forkhead box, sub-group O (FOXO) family of transcription factors (Glass, 2005). *In vitro* mechanical stretch mimics the effects of resistance exercise (Powell *et al.*, 2002) and has been used to investigate the influence of mechanical load on myotube protein synthesis (Vandenburgh *et al.*, 1989) and more recently, Akt activation (Hornberger *et al.*, 2005). However, whether mechanical stretch causes an increase in protein synthesis *via* Akt signalling has not been determined. This study aimed to determine whether the increase in Akt signalling seen in response to ten minutes of stretch (Hornberger *et al.*, 2005) results in an increase in protein synthesis, and whether the increase in protein synthesis seen in response to 48 hours of stretch (Vandenburgh *et al.*, 1989) was associated with an increased activation of the Akt signalling pathways.

Methods. C2C12 myoblast cultures were grown and differentiated into myotubes on Bioflex 6-well flexible bottom culture plates. Myotubes were mechanically stretched using the Flexcell strain unit (FX-4000) for either 10 min at 15% stretch (Hornberger *et al.*, 2005) or 48 h at 8% stretch (Vandenburgh *et al.*, 1989). Phosphorylated and total proteins for Akt, p70S6k, GSK-3β, and FOXO were measured using western blotting techniques. Atrogin-1 and MuRF1 mRNA levels were measured using real time-PCR. Protein synthesis rates were measured by the incorporation of [^{3}H]-tyrosine into the myotubes.

Results. Ten minutes of stretch caused an increase in phosphorylated Akt, p70S6k and GSK-3β and a decrease in Atrogin-1 and MuRF1 mRNA when measured immediately post-stretch. Protein synthesis rates, measured during the first 2 h post stretch, did not change. 48 h of stretch resulted in a decrease in phosphorylated Akt, p70S6k and GSK-3β as well as Atrogin-1 when measured immediately post-stretch. This was associated with a 12% increase in synthesis rates, measured during the last 2 h of stretch.

Conclusion. Short duration high-intensity mechanical stretching increases the phosphorylation of members of the Akt signalling pathway, but does not result in increases in protein synthesis within 2 h post stimulation. A longer time period of protein synthesis may be required. In contrast, longer duration low-intensity mechanical stretching results in a decrease in the phosphorylation of members of the Akt signalling pathway, but does result in increased protein synthesis during the last two hours of stimulation. The reduction in Akt signalling may be caused by a feed-back mechanism aimed at minimising excessive protein synthesis levels.

Glass, DJ. (2005) *International Journal of Biochemisty and Cell Biology* **37**, 1974-1984.

Hornberger TA, Armstrong DD, Koh TJ, Burkholder TJ & Esser KA. (2005) *American Journal of Physiology - Cell Physiology* **288**, C185-194.

Powell CA, Smiley BL, Mills J & Vandenburgh HH. (2002) *American Journal of Physiology - Cell Physiology* **283**, C1557-1565.

Vandenburgh HH, Hatfaludy S, Karlisch P & Shansky J. (1989) *American Journal of Physiology - Cell Physiology* **256**, C674-682.

Are genuine changes in protein expression being overlooked? Avoiding pitfalls in Western blotting quantification using AMPK and calsequestrin 1 as the proteins of interest

J.P. Mollica,[1] J.S. Oakhill,[2] G.D. Lamb[1] and R.M. Murphy,[1] [1]Department of Zoology, La Trobe University, Melbourne, VIC 3086, Australia and [2]St Vincent's Institute of Medical Research, Fitzroy, VIC 3065, Australia.

Western blotting has long been used in skeletal muscle physiology and biochemistry to examine relative amounts of specific proteins between treatment groups. An underlying assumption is that a linear, directly proportional, response exists between the amount of sample loaded and the density obtained for the protein band(s) of interest. Such a relationship does not usually exist and the present study highlights inadequacies in analysing proteins using arbitrary density units without the use of internal reference standard curves. It demonstrates that in order to correctly estimate relative changes in protein amounts, it is essential to establish the amount of sample that needs to be used and quantify the dynamic range over which the protein of interest can be detected.

Male Long-Evans hooded rats (6-8 months old) were sacrificed using a lethal overdose of fluothane in accordance with the La Trobe University Ethics Committee and the extensor digitorum longus (EDL) muscles excised. Whole muscle homogenates were used, that is, muscle samples were not subject to any centrifugation prior to Western blotting, in order to ensure that the entire pool of muscle proteins were represented. By ensuring that no proteins were inadvertently spun out, the absolute amounts of given proteins were able to be determined. A very sensitive Western blotting technique was used to detect calsequestrin 1 (CSQ1) and AMP kinase (AMPK) in as little as 2 μg total muscle homogenate (< 0.5 μg total protein). Using an anti-AMPK β1 isoform antibody, the concentration of AMPK in rat EDL muscle was determined to be ~60 μM. Standard curves prepared from both homogenates and pure protein samples of CSQ1 and AMPK demonstrated that loading too much sample (homogenates or pure proteins) would hinder seeing the true changes caused by some intervention, because the standard curves were no longer proportional with the amount of sample loaded (see Figure). This occurred with ~50 μg total muscle (~12 μg total protein) and 20 μg (~5 μg total protein) for CSQ1 and AMPK, respectively.

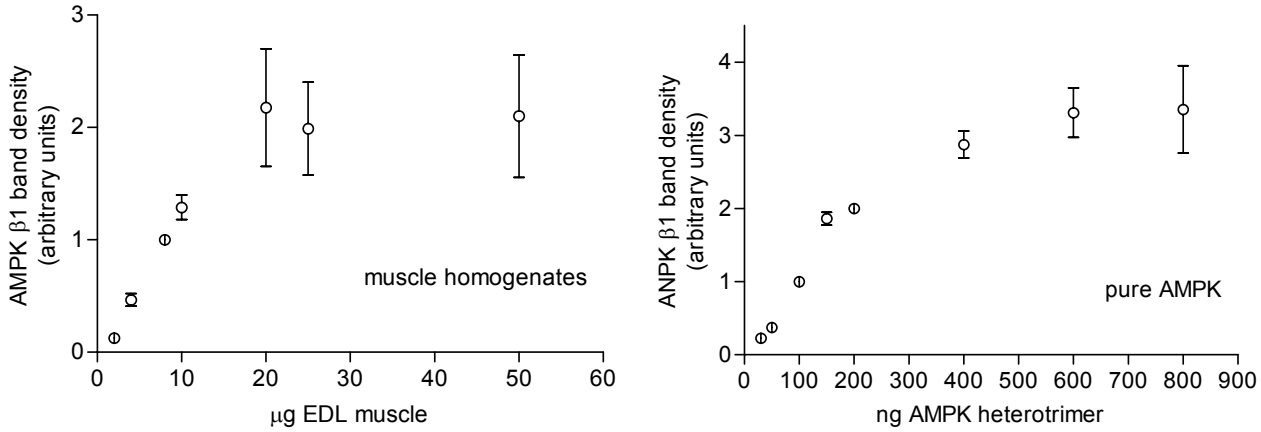

It was found, that extrapolation from a standard curve which although linear was not directly proportional, could result in an error of at least four-fold. This finding suggests the possibility that true changes due to a given treatment or intervention are not being detected. In conclusion, a simplistic approach of "less is more", (*i.e.* using small amounts of sample) enables a much clearer and more accurate outcome when using Western blotting for either absolute or relative amounts of particular proteins.

Properties of Heat Shock Protein 25 and 72 in rat skeletal muscle

N.T. Larkins, R.M. Murphy and G.D. Lamb, Department of Zoology, La Trobe University, Melbourne, VIC 3086, Australia.

Skeletal muscle has a remarkable ability to adapt to physiological stresses. Stresses such as glycogen depletion, myoplasmic free Ca^{2+} accumulation, ischemia, heat and exercise can all induce a family of proteins known as heat shock proteins (Hsp). These proteins are considered to play an essential role in maintaining cellular homeostasis through their role as molecular chaperones. These proteins are categorized by their molecular weights and show a high degree of homology among various species. The function and properties of Hsp 25 and Hsp 72 in non-stressed muscle are not well understood. In the present study we have assessed the relative and absolute amounts of Hsp 25 and Hsp 72 as well as their diffusibility and fibre type dependency in resting rat skeletal muscle.

Male Long-Evans hooded rats (6-8 months old) were sacrificed using a lethal overdose of Fluothane in accordance with the La Trobe University Ethics Committee and the extensor digitorum longus (EDL) and soleus (SOL) muscles were excised. Portions of muscle were homogenized and whole muscle homogenates were analysed using a sensitive Western blotting technique. To compare fibre type differences EDL (exclusively type II) and SOL (predominantly type I) muscles homogenates were run side by side. To determine the absolute amounts of Hsp 25 and 72 in muscle, known amounts of pure Hsp 25 and Hsp 72 were run on Western blots alongside the muscle homogenates samples (Murphy *et al.*, 2008). To measure protein diffusibility individual fibres were dissected from muscles that had been immersed in paraffin oil and then mechanically-skinned and exposed to physiological K^+-based solution (pCa < 10) for various times (2-120 mins). The wash solution and their matched fibres were analysed by Western blotting (Murphy *et al.*, 2006).

When equal amounts of whole EDL and SOL homogenates were compared, there was 2-3 times more Hsp 25 and Hsp 72 in SOL compare to EDL muscle homogenate. The absolute amounts of Hsp 25 and Hsp72 in SOL muscle were found to be ~5μM and ~2.6 μM, respectively. After mechanically-skinning SOL and EDL fibres, ~two-thirds of Hsp 25 and Hsp 72 were found in the wash solutions, indicating these proteins are essentially free to diffuse within the cytoplasm.

Murphy RM, Larkins NT, Mollica JP, Beard NA, Lamb GD. (2008) *Journal of Physiology*, submitted.
Murphy RM, Verburg E, Lamb GD. (2006) *Journal of Physiology*, **576:** 595-612.

Attenuation of glucose uptake is associated with reduced levels of striated activator of Rho signalling (STARS) in L6 myotubes

M.A. Wallace and A.P. Russell, The Centre for Physical Activity and Nutrition Research (C-PAN), School of Exercise and Nutrition Sciences, Deakin University, VIC 3215, Australia.

Introduction. STARS is a novel actin-binding protein specifically expressed in cardiac and skeletal muscle (Arai *et al.*, 2002). STARS binds to the I-band of the sarcomere and to actin where, in part collaboration with RhoA, stimulates the binding of free G-actin to F-actin filaments, resulting in enhanced actin polymerization and/or stabilization. The reduction in the pool of free G-actin removes its inhibition of the transcriptional co-activator myocardin-related transcription factor-A (MRTF-A) (Sotiropoulos *et al.*, 1999); the latter a positive regulator of serum response factor (SRF) transcriptional activity (Miralles *et al.*, 2003). Actin polymerization is also associated with increased skeletal muscle glucose uptake (Kanzaki, 2006). High levels of palmitic acid (PA) can cause apoptosis and attenuate glucose uptake (Turpin *et al.*, 2006), however whether this is associated with a reduction of STARS and actin polymerization is unknown.

Methods. Differentiated L6 muscle cells were treated with or without 0.75mM PA for 24 hours, followed by stimulation with or without 10 nM insulin for 30 minutes. Glucose uptake was determined by measuring the uptake of C^{14}-2-Deoxy-D-glucose (2-DG). STARS mRNA was measured using qPCR. Statistical analyses were performed using a one-way ANOVA.

Results. As shown in the figure PA reduced both basal and insulin stimulated 2-DG uptake ($p<0.05$) with a concomitant reduction in STARS mRNA ($p<0.01$).

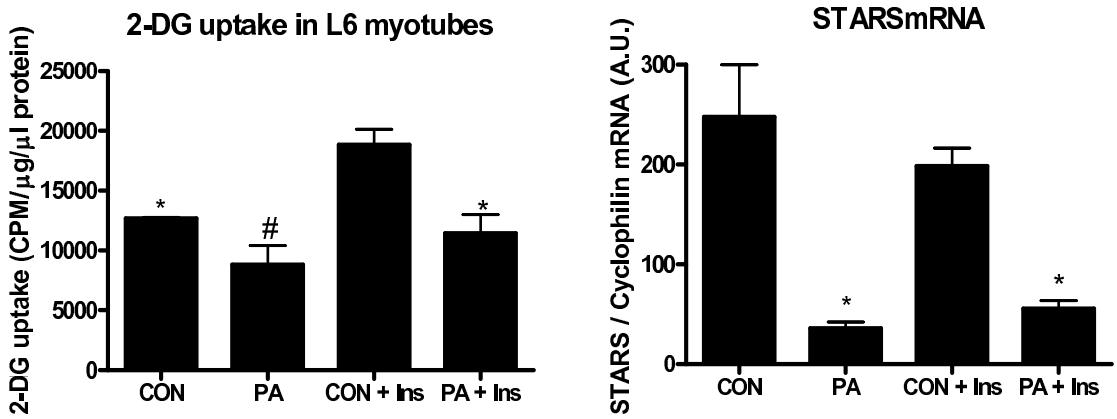

Conclusions. PA-induced reduction in 2-DG uptake is associated with a decrease in STARS mRNA in L6 muscle cells. By analogy, the reduced level of STARS indicates a decrease in actin polymerization, MRTF translocation and SRF transcription. These results suggest that STARS signalling might play a role in basal and insulin stimulated glucose uptake. Future studies are required to establish if the down regulation of STARS has a causal influence on glucose uptake and insulin sensitivity in skeletal muscle.

Arai, A, Spencer, JA & Olson, EN. (2002). *Journal of Biological Chemistry,* 277, 24453-24459.
Kanzaki, M. (2006). *Endocrinology Journal*, 53, 267-293.
Miralles, F, Posern, G, Zaromytidou, AI & Treisman, R. (2003). *Cell* 113, 329-342.
Sotiropoulos, A, Gineitis, D, Copeland, J & Treisman, R. (1999). *Cell* 98, 159-169.
Turpin, SM, Lancaster, GI, Darby, I, Febbraio, MA & Watt, MJ. (2006). *American Journal of Physiology - Endocrinology and Metabolism,* 291, E1341-1350.

The effect of estrogen on Akt signalling and protein synthesis in C2C12 mouse skeletal myotubes

R.J. Stefanetti, A.I. Turner, M.J. Quick, R.J. Snow and A.P. Russell, The Centre for Physical Activity and Nutrition Research (C-PAN), School of Exercise and Nutrition Sciences, Deakin University, VIC 3125, Australia.

The maintenance of skeletal muscle mass is a critical component of health in both chronic wasting diseases and aging. A considerable amount of progress has been made in the understanding of the signalling pathways that mediate skeletal muscle hypertrophy and atrophy. Akt is seen as a key molecular protein involved in the maintenance of skeletal muscle mass as it has the dual ability to positively influence protein syntheses and negatively regulate protein degradation in its active state (Glass, 2003). Potential mechanisms which may assist with maintaining skeletal muscle mass are the estrogen hormones. Estrogens increase the proliferation of mouse and rat myoblasts and can also attenuate immobilization-induced skeletal muscle atrophy in rats *in vivo* (Kahlert *et al.*, 1997). No studies have investigated the effect of estrogens on the activation of skeletal muscle hypertrophy and atrophy signalling pathways. Estrogens may contribute to maintaining skeletal muscle mass *via* their activation of the Akt signalling pathways. Therefore, the aims of the present study were to determine if treatment of C2C12 myotubes with either 17β-estrodiol or estrone increases the activity of Akt and its downstream anabolic signalling proteins, GSK, p70s6k and 4E-BP1 and decreases its catabolic stimulating targets, FOXO, atrogin-1 and MuRF-1. A secondary aim was to determine if this was associated with an increased rate of protein synthesis.

C2C12 myotubes were incubated at 37°C in serum free DMEM without phenol red containing 10 000 units/ml penicillin, 10 000 μg/ml streptomycin, and 250μg/ml amphotericin B for 24h. Myotubes were then stimulated with 17-β estradiol (10nM) for 24h. Phosphorylated and total proteins for Akt, p70S6k, GSK3β, 4E-BP1, FOXO and atrogin-1 were measured using western blotting techniques. Atrogin-1 and MuRF1 mRNA levels were measured using real time-PCR. Protein synthesis rates were measured by incorporation of [^{3}H]-tyrosine into the myotubes during the last hour of treatment.

Compared to control myotubes, treatment with 17β-estradiol increased the ratio of phosphorylated to total protein contents for Akt, GSK-3β and P70^{s6k} by, 1.62, 1.53 and 2.2 fold, respectively (n=6 per group; $p < 0.05$). There was, however, no difference in the ratios of phosphorylated to total 4E-BP1 or Foxo3a or Atrogin-1 and MuRF1 mRNA. Protein synthesis rates remained unchanged.

This study demonstrates that in C2C12 mouse myotubes, 17β-estradiol treatment increases the phosphorylation of the hypertrophy signalling protein, Akt, and its downstream hypertrophy signalling targets, GSK-3β and P70^{s6k}; no associated changes in protein synthesis were observed. Future studies should investigate the ability of 17β-estradiol to activate these proteins in a model of myotube catabolism and to determine if protein degradation is attenuated.

Glass DJ. (2003) *Nature Cell Biology*, **5**, 87-90.

Kahlert S, Grohe C, Karas RH, Lobbert K, Neyses L. Vetter H. (1997) *Biochemical and Biophysical Research Communications*, **232**, 373-378.

The relative amounts of PTEN protein in rat cardiac and skeletal muscles and the effect of high dose statins

C.A. Goodman, H. Yue, D.J. Pol and G.K. McConell, Department of Physiology, The University of Melbourne, Parkville, VIC 3010, Australia.

The tumor suppressor PTEN (phosphatase and tensin homologue deleted from chromosome 10) is a dual protein and lipid phosphatase which negatively regulates the PI3K/AKT pathway thus affecting metabolism and growth. Muscle specific deletion of Pten enhances insulin-stimulated glucose uptake in mouse slow twitch soleus but not in fast twitch EDL muscle (Wijesekara *et al*., 2005). To date, few studies have examined PTEN protein expression in rat muscle and no studies have examined the relative expression of PTEN across muscles with different fiber type compositions and different functions. Two previous studies have shown that prolonged statin [3-hydroxy-3-methylglutaryl coenzyme A (HMG-CoA) inhibitors] administration leads to increased PTEN protein levels in the heart (Planavila *et al*., 2008; Mensah *et al*., 2005) possibly via increased PPAR-γ mediated transcription (Teresi, *et al*., 2008). Others have shown that PPAR-γ agonists lead to reduced muscle PTEN levels (Kim *et al*., 2007). No studies have examined the effect of high dose statins on skeletal muscle PTEN protein expression. Therefore the aim of this study was to investigate: 1) the relative content of PTEN protein in cardiac and skeletal muscles of different fibre types and 2) the effect of prolonged high dose statin administration on PTEN protein expression in the tibialis anterior muscle.

Twenty four male Sprague Dawley rats (6-7 wks) were divided into three groups: 1) controls, 2) 60 $mg \cdot kg^{-1} \cdot d^{-1}$ simvastatin and 3) 80 $mg \cdot kg^{-1} \cdot d^{-1}$ simvastatin. All rats had *ad libitum* access to food and water. Rats were orally gavaged daily for 14 days with either a vehicle (0.5% methyl cellulose) or simvastatin + vehicle at a constant relative volume of $5ml \cdot kg^{-1}$ body mass. On day 15, rats were killed with an overdose of pentobarbitone (0.7ml of pentobarbital sodium-$325mg \cdot ml^{-1}$) and the heart and soleus, EDL, plantaris and tibialis anterior muscles rapidly dissected. Pten protein was analysed by western blot with the density of the PTEN protein band expressed relative to the amount of protein loaded onto each gel (60μg). Results are Mean ± SE. Statistical analysis performed with one-way ANOVA with Bonferoni post-test. Significance at $p < 0.05$.

Under control conditions, the PTEN antibody detected two protein bands in the heart samples suggestive of two different isoforms but only one band in all the skeletal muscles. The amount of PTEN protein in control muscles was greater ($p < 0.05$) in the heart (0.149 ± 0.009 A.U./μg protein; n = 8) compared to the skeletal muscles, with soleus (0.074 ± 0.002 A.U./μg protein) and tibialis anterior (0.089 ± 0.004 A.U./μg protein; n = 8) having greater amounts of PTEN than EDL (0.047 ± 0.007 A.U./μg protein; n = 8) and plantaris (0.047 ± 0.002 A.U./μg protein; n = 8) which were not different from each other ($p > 0.05$). Two weeks of either 60 $mg.kg^{-1} \cdot d^{-1}$ or 80 $mg \cdot kg^{-1} \cdot d^{-1}$ group resulted in 10.2% and 20.5% less body weight ($p>0.05$) gain compared to controls ($p < 0.05$). Neither 60 or 80 $mg \cdot kg^{-1} \cdot d^{-1}$ of simvastatin for 14 days resulted in a change in the amount of PTEN protein in the tibialis anterior muscle compared to Control muscles (0.368 ± 0.016 *vs* 0.361 ± 0.011 *vs* 0.410 ± 0.027 A.U./μg protein, respectively).

In conclusion, rat PTEN protein levels vary between cardiac and skeletal muscle and between skeletal muscles of different fibre types. In addition, in contrast to previous studies in cardiac muscle, prolonged statin administration did not alter skeletal muscle levels of PTEN protein.

Kim KY, Cho HS, Jung WH, Kim SS & Cheon HG (2007) *Molecular Pharmacology* **71**, 1554-1562.

Mensah K, Mocanu MM, Yellon DM. (2005) *Journal of the American College of Cardiology* **45**, 1287-1291.

Planavila A, Rodríguez-Calvo R, Palomer X, Coll T, Sánchez RM, Merlos M, Laguna JC, Vázquez-Carrera M. (2008) *Biochimica et Biophysica Acta* **1781**, 26-35.

Teresi RE, Planchon SM, Waite KA, Eng C. (2008) *Human Molecular Genetics* **17**, 919-928.

Wijesekara N, Konrad D, Eweida M, Jefferies C, Liadis N, Giacca A, Crackower M, Suzuki A, Mak TW, Kahn CR, Klip A, Woo M. (2005) *Molecular and Cellular Biology* **25**, 1135-1145.

Myostatin inhibition increases muscle mass in adult *mdx* dystrophic mice but does not enhance regenerative capacity of dystrophic skeletal muscle after injury

S.M. Snell, K.T. Murphy, R. Koopman and G.S. Lynch, Basic and Clinical Myology Laboratory, Department of Physiology, The University of Melbourne, Victoria 3010, Australia.

Duchenne muscular dystrophy (DMD) is characterised by continuous cycles of muscle fibre degeneration with less than successful fibre regeneration, leading to progressive muscle wasting, weakness and premature death. There is a profound need to identify therapeutic strategies to improve the dystrophic pathology and enhance quality of life for these patients. Myostatin, a member of the transforming growth factor-β (TGF-β) superfamily, is a negative regulator of muscle mass; high levels of myostatin suppress muscle growth whereas lower levels promote muscle growth (McPherron *et al.*, 1997). Thus, myostatin blockade represents a potential strategy to improve the regenerative capacity and function of dystrophic skeletal muscles. We tested the hypothesis that myostatin inhibition in adult *mdx* mice, a commonly used animal model of DMD, would improve the regenerative capacity and enhance function of dystrophic skeletal muscle.

Male C57Bl/10ScSn *mdx*/J (*mdx*; 12 week old; n=55) mice received weekly subcutaneous injections of either saline or a myostatin antibody (developed by Pfizer Inc., USA; 10 mg/kg) for up to 8 weeks. Five weeks after commencing treatment, mice were anaesthetized deeply (Ketamine, 76 mg/kg, Xylazine, 10 mg/kg, *i.p.*) and the *tibialis anterior* (TA) muscle of the right hindlimb injected with the myotoxin Notexin (~40-50μl; 1 μg/ml in 0.9% saline), to induce complete muscle fibre degeneration. Maximal force production of regenerating muscles was determined at 7, 14, 21 or 28 days post-injury using an *in situ* approach. In addition, for the 28 day post-injury group, the diaphragm was excised from deeply anaesthetized animals (sodium pentobarbital, 60 mg/kg, *i.p.*) and function of isolated diaphragm muscle strips assessed *in vitro* according to methods described in detail previously (Lynch *et al.*, 1997). All mice were killed *via* cardiac excision, while under deep anaesthesia.

The body mass of myostatin antibody treated mice was 13% and 10% greater than that of control mice at 14 and 21 days, respectively ($p < 0.05$). The mass of injured/regenerating TA muscles was greater in the antibody treated group compared with control at 7, 14 and 21 days post-injury ($p < 0.05$), but not at 28 days post-injury. Despite the increase in muscle mass in antibody treated mice, there was no difference in absolute or specific (normalised) force production between groups. There was no difference in specific force production of diaphragm strips between treated and control mice nor did treatment confer protection from contraction-mediated injury, based on muscle force responses during a protocol of repeated lengthening contractions (as described by Schertzer *et al.*, 2007). These data demonstrate that inhibiting myostatin can increase muscle mass in adult *mdx* mice but this may not necessarily translate to an increase in maximal force production.

Lynch, G.S., Rafael, J.A., Hinkle, R.T., Cole, N.M., Chamberlain, J.S. & Faulkner, J.A. (1997). *American Journal of Physiology* **272**, C2063-C2068.

McPherron, A.C., Lawler A.M. & Lee, S-J. (1997). *Nature* **387**, 83-90.

Schertzer J.D., Gehrig S.M., Ryall J.G. & Lynch, G.S. (2007). *American Journal of Pathology* **171**, 1180-88.

Supported by research grant funding from Pfizer Inc. (USA).

Macrophage polarization induced by different toll-like receptor agonists mediate insulin responses in muscle cells

J.D. Schertzer, V. Samokhvalov, P.J. Bilan, C.N. Antonescu and A. Klip, Cell Biology Program, The Hospital for Sick Children, Toronto, ON, M5G 1X8, Canada.

Skeletal muscle is the main site of postprandial glucose disposal and defects in muscle glucose transport are critical in the development of type 2 diabetes. Diets inappropriately high in saturated fat are associated with a state of chronic inflammation and contribute to insulin resistance. Recent evidence had implicated toll-like receptors (TLRs), components of the innate immune system, in propagating fatty acid-induced inflammatory signals leading to insulin resistance. Direct exposure of muscle cells to palmitate, one of the most abundant dietary saturated fats, causes insulin resistance, an effect associated with signaling through TLRs. Bacterial infection is also associated with insulin resistance and direct administration of lipopolysaccharide (LPS), a wall component of Gram-negative bacteria and well-known TLR4 agonist, can cause insulin resistance. Macrophage-adipose cell cross-talk has been implicated in fatty-acid induced inflammation and insulin resistance, but the role of macrophage secreted factors on insulin responses in muscle cells is ill-defined. We hypothesized that conditioned medium from palmitate and LPS treated macrophages would cause insulin resistance in muscle cells. Treating RAW264.7 macrophages with 0.5 mM palmitate for 6 h increased the expression of inducible nitric oxide synthase (iNOS) by ~3-fold and did not alter the expression of arginase. Conditioned medium from palmitate-treated macrophages inhibited insulin-stimulated glucose uptake and GLUT4 translocation in L6-GLUT4*myc* muscle cells. This suggests that palmitate promotes macrophage polarization towards the M1 pro-inflammatory state, which can lead to the release of factors that cause insulin resistance in muscle cells. Contrary to our hypothesis, treating macrophages with 10 ng/mL of LPS for 24 hours increased the expression of arginase by ~4-fold and increased iNOS expression by ~3-fold, suggesting a polarization of these macrophages towards the M2 anti-inflammatory state. Moreover, conditioned medium from LPS-treated macrophages stimulated insulin-induced glucose uptake and GLUT4 translocation in L6-GLUT4*myc* muscle cells. Importantly, analysis of differences in macrophage secreted factors revealed that LPS induced a 16-fold increase in the anti-inflammatory cytokine, IL-10, whereas palmitate treatment only increased IL-10 by 2-fold. Exogenous IL-10 stimulated insulin action in muscle cells and attenuated insulin resistance caused by conditioned medium from palmitate-treated macrophages. These results indicate that macrophages may be an integral element linking inflammation and glucose homeostasis in skeletal muscle. Our data suggests that the polarization state of macrophages, which can be differentially regulated by innate immune responses to saturated fatty acids or LPS, can impinge or potentiate insulin responses in skeletal muscle cells.

Support: Natural Sciences and Engineering Research Council of Canada, Canadian Institutes of Health Research and Canadian Diabetes Association.

Identifying the site of the source of reactive oxygen species within the mitochondria after transient exposure of cardiac myocytes to hydrogen peroxide

H.M. Viola,[1] E. Ingley,[2] P.G. Arthur[1] and L.C. Hool,[1] [1]School of Biomedical, Biomolecular and Chemical Sciences, University of Western Australia, Crawley, WA 6009, Australia and [2]Western Australian Institute for Medical Research, Perth, WA 6000, Australia.

Oxidative stress is a feature of cardiovascular disease and hydrogen peroxide (H_2O_2) can act as a signaling molecule to mediate cardiovascular pathology. We have previously demonstrated that transient exposure of ventricular myocytes to H_2O_2 leads to a further increase in reactive oxygen species (ROS) from the mitochondria (supporting the "ROS-induced ROS-release" hypothesis). Exposure of cardiac myocytes to 30μM H_2O_2 for 5 min followed by 10U/ml catalase for 5 min to degrade the H_2O_2 caused a 65.4 ± 8.4% further increase in superoxide by the mitochondria (n = 47) (Viola *et al.*, 2007). NADPH-oxidase, xanthine oxidase and nitric oxide did not contribute to the increase in superoxide. We tested whether a transient exposure to H_2O_2 altered protein synthesis in the myocytes. Ventricular myocytes were isolated from hearts excised from anesthetised guinea pigs. We found that 5 min exposure to 30μM H_2O_2 followed by 10U/ml catalase for 5 min caused a two fold increase in protein synthesis measured as ^{3}H-Leucine incorporation (n = 10). This suggests that a transient exposure to H_2O_2 may be sufficient to induce cardiac hypertrophy. We wished to identify the site of the source of ROS in the mitochondria. Previous studies have shown the main source of ROS production by the mitochondria occurs via complex III although complex I may also be a source of ROS production (Turrens, 1997; St-Pierre *et al.*, 2002; Muller *et al.*, 2003; Turrens, 2003). We exposed myocytes to 1μM DPI, which binds just prior to the ROS generation site of complex I, followed by 30μM H_2O_2 for 5 min and 10U/ml catalase for 5 min. Superoxide was assessed with the fluorescent indicator dihydroethidium (DHE). The presence of DPI completely attenuated the increase in DHE after exposure to H_2O_2. We also exposed guinea pig cardiac myocytes to 1μM rotenone, which binds just after the ROS generation site of complex I, followed by 30μM H_2O_2 for 5 min and 10U/ml catalase for 5 min. The presence of rotenone attenuated the increase in DHE after exposure to H_2O_2 by 45%. These data suggest that the source of production of ROS is distal to complex I. Identifying the site of production of ROS may represent a possible therapeutic target to prevent the development of cardiac hypertrophy associated with a transient exposure to H_2O_2.

Muller FL, Roberts AG, Bowman MK & Kramer DM. (2003) *Biochemistry* **42:** 6493-9.
St-Pierre J, Buckingham JA, Roebuck SJ & Brand MD. (2002) *Journal of Biological Chemistry* **277:** 44784-90.
Turrens JF. (1997) *Bioscience Reports* **17:** 3-8.
Turrens JF. (2003) *Journal of Physiology* **552:** 335-44.
Viola HM, Arthur PG & Hool LC. (2007) *Circulation Research* **100:** 1036-44.

Comparison of the cardiac-specific effects of dietary omega-3 and omega-6 polyunsaturated fatty acids in male and female rats

A.P. McAlindon, J.R. Bell, C.L. Curl, C.E. Huggins and L.M.D. Delbridge, Cardiac Phenomics Laboratory, Department of Physiology, The University of Melbourne, VIC 3010, Australia.

Clinical trials have demonstrated that omega-3 polyunsaturated fatty acids (PUFA) reduce sudden death in patients with recent myocardial infarction (Burr *et al.,* 1989). Experimental studies provide further evidence of a cardioprotective role of omega-3 PUFA mediated through antiarrhythmic actions and altered Ca^{2+} handling. Whether these effects may be attributed to membrane-incorporated and/or free diffusible PUFA is controversial (Den Ruijter *et al.,* 2008). Furthermore, epidemiologic, clinical and experimental studies have almost exclusively focused on males. Given there are reported sex-related differences in cardiac function, and that these differences involve altered Ca^{2+} handling, it is surprising that the question of whether significant cardioprotection in the female heart can be achieved through dietary PUFA has not yet been explored. This experimental study investigated the sex-specific cardiac effects of dietary omega-3 (ω3) and omega-6 (ω6) PUFA.

Six-week old male and female Sprague Dawley rats were fed a fully fabricated isoenergetic diet high in either ω3 (N3D, Nu-Mega fish oil) or ω6 (N6D, sunflower oil) PUFA for eight weeks. At feeding completion, rats were anaesthetised with pentobarbitone sodium (20 mg/kg, IP), hearts rapidly excised and assigned to one of two experimental protocols. In an *ex vivo* study, hearts were perfused in Langendorff mode with oxygenated (95% O_2, 5% CO_2) bicarbonate buffer (37°C) at a constant pressure. Left ventricular pressure was measured continuously with an isovolumetric, intraventricular balloon inflated to produce an end diastolic pressure of 4 mmHg. *Ex vivo* functional parameters were determined following 30 minutes aerobic perfusion. In an *in vitro* study, hearts were perfused in Langendorff mode with 50 mg/ml collagenase to enzymatically disperse cardiomyocytes. Isolated myocytes were loaded with the Ca^{2+} indicator Fura-2 and placed in a superfusion chamber on the stage of an inverted fluorescence microscope. Fura-2 fluorescence (ratio 380/365nm) and cell shortening (edge detection) were monitored using an IonOptix fluorescence and contractility system (IonOptix Corporation, Maryland, USA). Cells were then superfused with 2mM Ca^{2+} HEPES-solution and paced at 4 Hz to examine basal functional parameters. All data are presented as mean ± SEM and analysed by two-way ANOVA.

We have previously shown that with these dietary interventions ω3 and ω6 PUFA enrichment of cardiac membranes is achieved. Somatic growth over the dietary period was equal for N3D and N6D groups and at feeding completion there were no significant differences in body mass between dietary groups within each sex. Body mass of female rats was significantly lower (male: N3D: 573 ± 14 g, N6D: 582 ±15 g; female: N3D: 303 ± 9 g, N6D: 327 ± 12 g; diet $p > 0.05$; sex $p < 0.05$, n = 9-12/diet group). There was no effect of diet on systolic blood pressure measured using tail cuff plethysmography, although pressure observed in female rats was significantly lower. No significant sex or diet differences were observed in basal left-ventricular developed pressure, heart rate, dP/dt max or min. A significant reduction in rate-pressure product was observed in N3D for both sexes (male: N3D: 30983 ± 2315 $mmHg.min^{-1}$, N6D: 37439 ± 897 $mmHg.min^{-1}$; female: N3D: 32513 ± 1815$mmHg.min^{-1}$, N6D: 35056 ± 1677 $mmHg.min^{-1}$; diet $p < 0.05$; sex p>0.05, n = 5-7/diet group). Myocyte diastolic Ca^{2+} was significantly lower in N3D groups (Ca^{2+} ratio; male: N3D: 1.79 ± 0.04, N6D: 2.00 ± 0.08; female: N3D: 1.73 ± 0.06, N6D: 1.86 ± 0.07; diet $p < 0.05$; sex $p > 0.05$, n = 6-11 cells/diet group). N3D groups also exhibited significantly reduced systolic Ca^{2+} (Ca^{2+} ratio; male: N3D: 2.03 ± 0.04, N6D: 2.33 ± 0.12; female: N3D: 1.92 ± 0.09, N6D: 2.21 ± 0.08; diet $p < 0.05$; sex $p > 0.05$, n = 3 hearts/diet group). Myocyte shortening was not significantly influenced by diet or sex, although there was a trend for female N3D myocytes to exhibit reduced shortening.

In summary, although minimal functional effect of N3D was observed under basal conditions in *ex vivo* perfused hearts, significant differences in Ca^{2+} handling were observed for myocytes of N3D and N6D groups. These results are the first to demonstrate altered Ca^{2+} handling in female cardiomyocytes as a result of dietary ω3 intervention. These results also provide evidence for membrane-incorporated ω3 PUFA to modulate cardiac function and cardiomyocyte calcium flux in both sexes. Further characterisation of the role of PUFA dietary intervention in modulation of myocardial function in females is warranted.

Burr ML, Fehily AM, Gilbert JF, Rogers S, Holliday RM, Sweetnam PM, Elwood PC, Deadman NM. (1989) *Lancet*, **2:** 757-61.

Den Ruijter HM, Berecki G, Verkerk AO, Bakker D, Baartscheer A, Schumacher CA, Belterman CNW, de Jonge N, Fiolet JWT, Brouwer IA, Coronel R. (2008) *Circulation*, **117:** 536-44.

Role of β-adrenoceptors during early skeletal muscle regeneration in mice

R. Sheorey, J.G. Ryall, J.E. Church and G.S. Lynch, Basic and Clinical Myology Laboratory, Department of Physiology, The University of Melbourne, VIC 3010, Australia.

Skeletal muscles can be injured via numerous physical, metabolic and thermal insults, leading to a loss of force production. A greater understanding of the processes controlling skeletal muscle regeneration may lead to novel treatments for muscle injuries and muscle diseases. We have previously identified the β-adrenoceptor (β-AR) signalling pathway as a potential regulator of muscle regeneration after injury (Beitzel *et al*. 2004; 2007). The aim of this study was to determine whether β-ARs are necessary for successful muscle fibre regeneration. Since transgenic mice lacking both β_1- and β_2-AR subtypes are available (*Adrb1*$^{-/-}$/*Adrb2*$^{-/-}$), we determined the physiological role of β-AR signalling during skeletal muscle regeneration after injury. We tested the hypothesis that mice homozygous null for β_1-ARs and β_2-ARs (*Adrb1*$^{-/-}$/*Adrb2*$^{-/-}$) would exhibit impaired muscle regeneration, as evidenced by reduced muscle function.

To examine the role of β-ARs in muscle regeneration, we utilized 7-8 week old *Adrb1*$^{-/-}$/*Adrb2*$^{-/-}$ mice (*n* = 27, Jackson Laboratory, USA, $Adrb1_{tm1Bkk}Adrb2_{tm1Bkk/J}$, stock no. 003810) and C57BL/6 wild-type mice (WT, *n* = 31, Animal Resource Centre, Canningvale, WA, Australia). Mice were anaesthetized deeply (ketamine 76 mg/kg and xylazine 10 mg/kg; *i.p.*) and the extensor digitorum longus (EDL, fast-twitch) muscle was surgically exposed and injected with Notexin (1μg/mL; Lotaxan, Valence, France) to cause complete degeneration of all muscle fibres (Plant *et al*. 2006). The contralateral EDL muscle served as the uninjured control in each case. Mice were allowed to recover for 7, 14 or 21 days, at which time they were anaesthetized deeply with sodium pentobarbitone (60 mg/kg; *i.p.*) and isometric contractile properties of injured and uninjured muscles were determined *in vitro*, as described previously (Plant *et al*. 2004). Mice were killed by cardiac excision while anaesthetized.

Maximum force was not different between uninjured EDL muscles from *Adrb1*$^{-/-}$/*Adrb2*$^{-/-}$ and WT mice ($234 \pm 5 kN/m^2$ and $238 \pm 7 kN/m^2$, respectively). The force producing capacity of muscles from WT mice at 7, 14 and 21 days post-injury was 31%, 64% and 78% of their uninjured control values, respectively. In contrast, the force producing capacity of muscles from *Adrb1*$^{-/-}$/*Adrb2*$^{-/-}$ mice at 7, 14 and 21 days post-injury was 3%, 64% and 78% of their uninjured controls, respectively.

Our findings indicate that while β-ARs are not required for successful skeletal muscle regeneration, as evidenced by the restoration of force producing capacity to uninjured control levels by 14 and 21 days post-injury, they may play an important (and previously unreported) role during early muscle regeneration. Clarification is required on the role of β-AR signalling on inflammatory and early myogenic processes such as myoblast differentiation and cell fusion. Our results suggest that manipulation of the β-AR signalling pathway during early regeneration after injury may improve the rate, extent and efficacy of these regenerative processes. The findings have important implications for the treatment of muscle wasting conditions especially muscle diseases where regeneration is defective.

Beitzel F, Gregorevic P, Ryall JG, Plant DR, Sillence MN, Lynch GS. (2004). *Journal of Applied Physiology*, **96:** 1385-92.

Beitzel F, Sillence MN, Lynch GS. (2007). *American Journal of Physiology Endocrinology and Metabolism*, **293:** E932-40.

Plant DR, Colarossi FE, Lynch GS. (2006). *Muscle & Nerve*, **34:** 577-85.

Supported by research grant funding from the National Health and Medical Research Council (509313).

Nitric oxide and skeletal muscle regeneration in mice after injury – the role of muscular nNOS

J.E. Church, S.M. Gehrig, G.K. McConell and G.S. Lynch, Basic & Clinical Myology Laboratory, Department of Physiology, University of Melbourne, VIC 3010, Australia.

Nitric oxide (NO) plays a complex role in skeletal muscle biology and its role, particularly in muscular regeneration, is still not fully understood. Increased NO in skeletal muscle has been reported to be beneficial in models of muscle injury and degeneration/regeneration such as muscular dystrophy (Wehling *et al.*, 2001) or crush injury (Anderson, 2000), but NO also plays a prominent role in the muscle wasting (or cachexia) associated with inflammatory disorders (Marinez-Moreno *et al.*, 2007). These seemingly contradictory effects of NO in skeletal muscle may be dictated by a combination of subcellular localisation and/or concentration of NO, both of which are intimately related to the isoform of nitric oxide synthase (NOS) from which the NO is produced. Although skeletal muscle can express all three subtypes of NOS (nNOS, eNOS and iNOS), nNOS is the most highly expressed isoform of NOS in skeletal muscle.

The aim of this study was to clarify the role of nNOS-derived NO in skeletal muscle by examining muscle fibre regeneration after myotoxic injury in mice genetically lacking nNOS. Twelve week old C57BL/6J-Nos1^{tm1Plh} mice homozygously null for the nNOS gene (nNOS$^{-/-}$) and their littermate controls (nNOS$^{+/+}$) were used in this study. Muscle function of the *tibialis anterior* (TA) muscle of the right hindlimb was assessed *in situ* using methods described in detail previously (Schertzer *et al.*, 2007). Maximal isometric force (P_o) was determined from the frequency-force relationship and muscle fatiguability determined from a protocol of repeated, intermittent isometric contractions.

TA muscles from nNOS$^{-/-}$ mice were less susceptible ($P < 0.05$) to fatigue than nNOS$^{+/+}$ mice but specific force (P_o normalised to muscle cross-sectional area, sP_o) and the frequency-force relationships were not different between groups. To examine the contribution of nNOS to muscle regeneration after injury, mice were anaesthetised (ketamine 100mg/kg and xylazine 10mg/kg; *i.p.*) and the TA muscle of the right hindlimb injected with the myotoxin Notexin (1μg/ml, *i.m.*) to cause degeneration of all muscle fibres. Mice were allowed to recover for 10 days, after which function of the TA muscle was assessed *in situ*. At 10 days post-injury, the sP_o of the regenerating TA muscles, while lower ($P < 0.05$) than that of uninjured muscles, was unchanged between the two groups. These findings suggest that expression of nNOS does not appear to be a critical factor in successful regeneration of skeletal muscle with this mode of injury.

Anderson, J.E. (2000) *Molecular Biology of the Cell*, **11,** 1859-1874.

Martínez-Moreno, M., Martínez-Ruiz, A., Alvarez-Barrientos, A., Gavilanes, F., Lamas, S. & Rodríguez-Crespo, I. (2007) *Journal of Biological Chemistry* **282,** 23044-23054.

Schertzer J.D., Gehrig S.M., Ryall J.G. & Lynch, G.S. (2007) *American Journal of Pathology* **171**, 1180-1188.

Wehling, M., Spencer, M.J. & Tidball, J.G. (2001) *Journal of Cell Biology*, **155,** 123-131.

Supported by the Muscular Dystrophy Association (USA)

Developmental changes in contractile function of the diaphragm in the pre-term lamb

T. Lavin,[1] J. Pillow,[2] A.J. Bakker,[1] C. McLean[2] and G.J. Pinniger,[1] [1]School of Biomedical, Biomolecular and Chemical sciences, and [2]School of Women and Infants Health, University of Western Australia, WA 6009, Australia.

The reduced force producing capacity and decreased fatigue resistance that arise from mechanical ventilation have been termed ventilator induced diaphragm dysfunction (VIDD). Although VIDD has been characterised in adults after mechanical ventilation, no study has systematically explored the existence of and pre-disposing factors to VIDD in the newborn subject. We propose that the functional development of the diaphragm may play a role in the onset of VIDD in neonates as gestational differences in transdiaphragmatic pressure and maximal inspiratory pressure have been observed (Dimitriou *et al.*, 2001). Developmental changes in the contractile function of the diaphragm have been examined primarily in small laboratory animals. However, most developmental changes in rodents occur *ex utero* while the majority of development in human neonates occurs *in utero* (Finkelstein *et al.*, 1992). Furthermore, the higher proportion of fast fibres and higher respiratory rate in small laboratory animals (Hodge *et al.*, 1997) may impact on the contractile properties of the diaphragm and therefore affect the susceptibility to damage, fatigue and VIDD. As little is known about the *in utero* development of fibre type composition and contractile properties of the diaphragm in human neonates, we used a comparable ovine animal model to investigate developmental changes in contractile function of the diaphragm at different gestational ages.

Fetuses of different ages were delivered at 75 days (n = 4), 100 days (n = 4), 128 days (n = 6) or 140 ± 2 days (n = 4) gestation or delivered at term (~150 days) and grown to 7 weeks postnatal age (200 day group; n = 4). The fetal diaphragm was removed after euthanasia via a lethal umbilical venous injection of pentobarbitone (100 mg/kg) and exsanguination via the femoral artery. Two strips of longitudinally arranged muscle fibres were dissected from the diaphragm muscle to assess 1) the susceptibility to muscle damage and 2) the recovery after fatigue. The rib and tendon ends of the muscle strip were tied with surgical silk and the preparation mounted in an *in vitro* muscle test system (1200A, Aurora Scientific Inc.) perfused with mammalian saline solution (in mM): NaCl (109), KCl (5), $MgCl_2$ (1), $CaCl_2$ (4), $NaHCO_3$ (24), NaH_2PO_4 (1), sodium pyruvate (10) and aerated with 95% O_2-5% CO_2 at 25°C. The contractile parameters were determined including maximum isometric tetanus (P_0), specific tetanic force (force/cross-sectional area, Sp_o), force-frequency relationship, maximum isomeric twitch force (P_t), time to P_t, half relaxation time, maximum rate of force development (dF/dt) before and after either a fatigue protocol (150 × 330 ms tetani trains, 80 Hz) or muscle damage protocol (5 × stretches at 10% fibre length during isometric plateau phase of Po). Fatigue index was calculated by dividing the 150th tetanic stimulus by the 1st tetanic stimulus during the fatigue protocol.

A number of significant (one-way ANOVA, bonferroni post-hoc, $p < 0.05$) age-dependant changes were seen, including: 1) three-fold increase in specific tetanic force from 75 d to 200 d (see Figure); 2) force frequency relationship increased by a factor of ~3 from 75 d to 200 d; 3) fatigue index decreased by half from 75 d to 200 d; 4) mean time to recovery after fatigue increased from 5 min at 75 d to 40 min at 200 d; 5) dF/dt decreased from 700 (g/s) at 100 d to 100 (g/s) at 200 d.

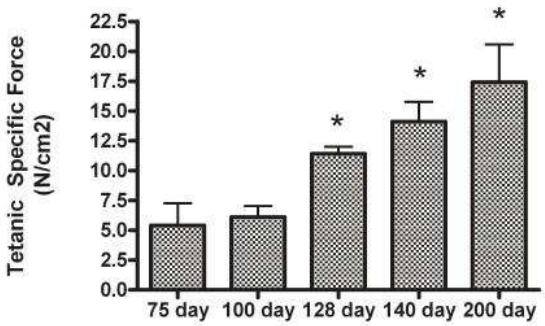

Mean and S.E. *p<0.05 compared with 75 day and 100 day groups

This study shows age-dependant changes in contractile function of the sheep diaphragm including increased Sp_0 and decreased fatigue resistance with advancing maturation. These changes may reflect a shift in fibre type composition from slow to fast fibres in the maturing diaphragm, or differences in the contractile function of fetal and neonatal muscle fibres. These data provide a framework from which we can investigate our hypothesis that the magnitude and nature of VIDD is influenced by gestation.

Dimitriou G, Greenough A, Rafferth GF & Maxham J. (2001) *American Journal of Respiratory and Critical Care Medicine*, **164:** 433-6.

Finkelstein DI, Andrianakis P, Luff AR & Walker DW. (1992) *American Journal of Physiology* **263:** 900-8.

Hodge K, Powers SK, Coombes J, Fletcher L, Demirel HA, Dodd SL, & Martin D. (1997) *Respiration Physiology*, **109:** 149-54.

Regulation of atrogin-1 and protein degradation following incubation with dexamethasone and TNFα in mouse C2C12 and primary human myotubes

A.E. Larsen, T.C. Crowe and A.P. Russell, The Centre for Physical Activity and Nutrition Research (C-PAN), School of Exercise and Nutrition Sciences, Deakin University, VIC 3125, Australia.

Introduction: Atrogin-1 is a muscle specific E3-ligase involved in muscle wasting (Bodine *et al.*, 2001). Increased levels of atrogin-1 mRNA has been observed in numerous *in vitro* and *in vivo* rodents models of muscle atrophy (Glass, 2005). Human studies performed have shown that atrogin-1 is increased in human atrophy conditions, such as leg immobilization (Jones *et al.*, 2004), ALS (Leger *et al.*, 2006), COPD (Doucet *et al.*, 2007) and quadriplegic myopathy (Di Giovanni *et al.*, 2004). In mice, but not humans, fasting increases atrogin-1 (Sandri *et al.*, 2004; Larsen *et al.*, 2006), suggesting that species differences may exists with respect to its regulation. The aim of the present study was to determine the regulation of atrogin-1 and protein degradation following treatment with dexamethasone (DEXA) and TNFα in mouse C2C12 and human primary myotubes.

Methods: Mouse C2C12 myotubes and primary human myotubes were treated with either TNF-α (20 ng/mL) or DEXA (10 μM) for 1, 4, 24 and 48-h. Atrogin-1 mRNA levels were measured using real time-PCR. Protein degradation was determined by measuring the release of [^{3}H]-tyrosine into the media.

Results: Atrogin-1 mRNA was significantly increased 2- and 4-fold in C2C12 myotubes after 24 and 48-h treatment with DEXA, respectively. In human myoblasts atrogin-1 was increased 2.2-fold only after 48-h of DEXA treatment. After treating C2C12 cells with TNF-α, atrogin-1 showed a transient change, increasing by 50% following 1-hr of treatment, decreasing to 50% below control levels following 4h of treatment then retuning to control levels after 24 and 48-h. In contrast, human myotubes treated with TNF-α showed a 3.1 fold increase in atrogin-1 after 48-h of treatment. In the human myotubes the increase in atrogin-1 mRNA levels following 48-h of both DEXA and TNF-α treatment resulted in significant increases in protein degradation by approximately 15%.

Conclusions: Treatment of both mouse C12C12 myotubes and primary human myotubes with DEXA results in increases in atrogin-1 mRNA; however human myotubes require a longer treatment period. Treatment with TNF-α demonstrated a more dramatic species dependent effect, with mouse C2C12 myotubes presenting a rapid increase, then decrease in atrogin-1 over 1-4 h of treatment, followed by a return to baseline lines at 48-h. In contrast, human myotubes had an increase in atrogin-1 mRNA 48- after treatment. In human myotubes the increases in atrogin-1 caused by both DEXA and TNF-α was associated with an increase in protein degradation. These observations highlight the need for caution when translating results obtained in rodent models to human conditions.

Bodine SC, Latres E, Baumhueter S, Lai VK, Nunez L, Clarke BA, Poueymirou WT, Panaro FJ, Na E, Dharmarajan K, Pan ZQ, Valenzuela DM, DeChiara TM Stitt, TN Yancopoulos GD, Glass DJ. (2001). *Science*, **294:** 1704-8.

Di Giovanni S, Molon A, Broccolini A, Melcon G, Mirabella M, Hoffman EP & Servidei S. (2004). *Annals of Neurology*, **55:** 195-206.

Doucet M, Russell AP, Leger B, Debigare R, Joanisse DR, Caron MA, Leblanc P & Maltais F. (2007). *American Journal of Respiratory and Critical Care Medicine*, **176:** 261-9.

Glass DJ. (2005). *International Journal of Biochemistry and Cell Biology*, **37:** 1974-84.

Jones SW, Hill RJ, Krasney PA, O'Conner B, Peirce N, Greenhaff PL. (2004) *FASEB Journal*, **18:** 1025-7.

Larsen AE, Tunstall RJ, Carey KA, Nicholas G, Kambadur R, Crowe TC, Cameron-Smith D. (2006). *Annals of Nutrition and Metabolism*, **50:** 476-81.

Leger B, Vergani L, Soraru G, Hespel P, Derave W, Gobelet C, D'Ascenzio C, Angelini C, Russell AP. (2006). *FASEB Journal*, **20:** 583-5.

Sandri M, Sandri C, Gilbert A, Skurk C, Calabria E, Picard A, Walsh K, Schiaffino S, Lecker SH, Goldberg AL. (2004) *Cell*, **117:** 399-412.

Store-dependent Ca^{2+} influx in intact healthy and dystrophic skeletal muscle

T.R. Cully,[1] O. Friedrich,[1] J.N. Edwards,[1,2] R.M. Murphy[2] and B.S. Launikonis,[1] [1]School of Biomedical Sciences, University of Queensland, St Lucia, QLD 4072, Australia and [2]Department of Zoology, La Trobe University, Melbourne, VIC 3086, Australia.

Store-operated Ca^{2+} entry (SOCE) is a mechanism that involves an extracellular Ca^{2+} influx in response to store-depletion to allow refilling of internal stores to physiological levels. It was suggested that SOCE may be enhanced in dystrophic skeletal muscle, activating proteolytic enzymes and triggering necrosis. However, those studies were exclusively performed in myotubes that do not compare to the fully differentiated muscle cell, where the dystrophic phenotype is primed. A recent study by Boittin *et al.*, (2006) claimed that SOCE flux rates were increased by an order of magnitude in adult single skeletal muscle fibres from dystrophic mdx mice compared to wild-type (wt). This SOCE flux rate was based on fluorescent myoplasmic signals from the high affinity Ca^{2+} dye fura-2. The plateau was reached within ~10 s in mdx, probably saturating the dye, and ~2 min in wt fibres. Having observed a robust and normally regulated SOCE in skinned fibres from mdx (Friedrich *et al.*, 2008), we re-examined SOCE fluxes in intact single wt and mdx muscle fibres.

C57BL/10 mice (8-20 weeks old) were killed by asphyxiation, in accordance to guidelines set by the Animal Ethics Committee of the University of Queensland. Interossei muscles were dissected and placed in a physiological saline. Isolated fibres were obtained by mild enzymatic treatment and loaded with 10 μM fluo-4AM (15 min) to allow for imaging of cytoplasmic Ca^{2+}. Sarcoplasmic reticulum $[Ca^{2+}]$($[Ca^{2+}]_{SR}$) was depleted by bathing the cells in a 0 Ca^{2+}, K^+-based physiological solution with 20 μM cyclopiazonic acid (CPA), followed by caffeine (10 mM) application. Fibres were then transferred into a 0 Ca^{2+}, Na^+-based solution containing Rhod-5N (10 μM) and 2 mM Ca^{2+} was added during imaging to measure SOCE. Fluorescence xyt images were obtained on an Olympus FV1000 confocal microscope. All solutions contained 50 μM BTS to prevent contraction.

After CPA incubation, caffeine evoked a significant fluorescence increase indicating that SR Ca^{2+} leakage alone does not fully deplete $[Ca^{2+}]_{SR}$. Therefore, all cells were depleted with CPA plus caffeine in a Ca^{2+}-free solution. By adding Ca^{2+} to the Rhod-5N containing solution, "Ca^{2+} arrival" at the depleted cell could be tracked. A very fast or very slow fluorescence increase was observed in response to SOCE regardless of cell type. The fast increase saturated the dye in ~50 s. All these cells vesiculated and were permeant to propidium iodide (PI). Thus, the high Ca^{2+} influx rates are a result of breakdown in membrane integrity. Cells that did not vesiculate also excluded PI entry and showed much slower fluorescence increases which did not saturate the dye. In these cells, there was three times larger SOCE flux into mdx compared to wt fibres. This result correlates well with increased expression of Stim1 and Orai1 in mdx compared to wt fibres (Friedrich *et al.*, 2008).

We conclude that there is an increased SOCE flux in dystrophic intact muscle that is, however, significantly lower than previously suggested (Boittin *et al.*, 2006). Furthermore, this increased influx will not contribute to Ca^{2+} overload in mdx cells due to the robust SOCE deactivation mechanism that persists in these cells (Friedrich *et al.*, 2008).

Boittin F, Petermann O, Hirn C, Mittaud P, Dorchies OM, Roulet E, Ruegg UT. (2006) *Journal Cell Science*, **119:** 3733-3742.

Friedrich O, Edwards JN, Murphy RM, Launikonis BS. (2008) *Proceedings of the Australian Physiological Society*, **39:** 19P.

Evidence of impaired store-operated Ca^{2+} entry in aged mammalian skeletal muscle

J.N. Edwards,[1,2] O. Friedrich,[1] T.R. Cully,[1] R.M. Murphy[2] and B.S. Launikonis,[1] [1]School of Biomedical Sciences, University of Queensland, St Lucia, QLD 4072, Australia and [2]Dept of Zoology, La Trobe University, Melbourne, VIC 3086, Australia.

Age-related effects on skeletal muscle function are increasingly recognized as contributing factors to a reduced lifestyle quality in the elderly population. Such effects include a decline in an individual's mobility and independence, possibly due to reduced specific force production and sarcopenia. As a major determinant of muscle force, it has been suggested that Ca^{2+} homeostasis is compromised in aged skeletal muscle (Delbono, 2002). Store-operated Ca^{2+} entry (SOCE) is a mechanism that involves extracellular Ca^{2+} entry in response to Ca^{2+} release from (and hence a reduction in) the intracellular Ca^{2+} stores. SOCE appears to be tailored to the specific needs of different cell types including highly specialized skeletal muscle cells (fibres); where force is produced in response to an increased myoplasmic [Ca^{2+}] due to Ca^{2+} release from the intracellular Ca^{2+} stores (sarcoplasmic reticulum, SR). Reduced SOCE and consequent cell function have been described in aged neuronal cells and aged fibroblasts. Thus, there is an importance to investigate SOCE in aged skeletal muscle because a change in Ca^{2+} handling through SOCE may contribute to the decline in force production.

Young (8-20 weeks) and aged (23 months) C57BL/10 mice were killed by asphyxiation, in accordance to the guidelines set by the Animal Ethics Committee of the University of Queensland. Tibialis anterior muscles were collected for protein analysis. Extensor digitorum longus muscles were rapidly excised, pinned out and fully immersed in paraffin oil. Small bundles of intact fibres were isolated and exposed to a Na^{+}-based physiological solution containing the fluorescent dye, fluo-5N salt. Single fibres were then isolated and mechanically skinned (resulting in the trapping of the dye in the t-system) and transferred to a chamber containing a K^{+}-based internal solution with 1 mM EGTA (100 nM free Ca^{2+}), 1 mM free Mg^{2+} and 50 μM rhod-2. Release of SR Ca^{2+} was evoked by substitution of the bathing solution with a 'low Mg^{2+}' solution, containing 0.01 mM Mg^{2+} and being nominally free of Ca^{2+}. Cytoplasmic rhod-2 and t-system fluo-5N were continuously imaged on an Olympus FV1000 confocal microscope in xyt mode during Ca^{2+} release at 1.0 NA. The net change in t-system fluo-5N signal was used as an indicator of SOCE activity (Launikonis and Ríos, 2007). The protein levels of Orai1 (the integral membrane Ca^{2+} channel thought to be responsible for SOCE) were measured in whole muscle homogenates by Western Blotting.

Substitution of the standard K^{+} -based intracellular solution with a low Mg^{2+} solution induced global SR Ca^{2+} release. This was accompanied by an initial Ca^{2+} uptake in the sealed t-tubules, followed by depletion due to SOCE. SOCE deactivation followed Ca^{2+} reuptake into the SR and reduction in myoplasmic Ca^{2+}. In some fibres, subsequent Ca^{2+} waves were observed, with defined fronts and defined onset of SOCE. This data, together with a high temporal resolution line acquisition, allowed the SOCE activation coupling delay to be measured (start of Ca^{2+} release wave until the beginning of SOCE). SOCE kinetics was analyzed by line-wise signal averaging with a 500Hz resolution. SOCE activation was significantly delayed in aged muscle (38 ± 3.1 ms, $n = 4$) compared to young mice (27 ± 3.6 ms, $n = 6$, $p = 0.044$). This data suggests that SOCE may be delayed in aged skeletal muscle and therefore compromise adequate fine tuning of store-refilling. This may be due to an approximately 50% reduction in Orai1 protein levels observed in aged skeletal muscle relative to skeletal muscle from young mice.

Delbono O. (2007) *Biogerontology*, **3:** 265-270.
Launikonis BS & Ríos E. (2007) *Journal of Physiology*, **583:** 81-97.

Examination of the expression of the cardiac muscle regulatory molecules, troponin T, I and C in the sheep heart across late gestation

G.S. Posterino,[1,3] S. Dunn,[2] K.J. Botting,[2,3] W. Wang,[2] H. Forbes[2] and J.L. Morrison,[2,3] [1]Department of Zoology, La Trobe University, Melbourne, VIC 8001, Australia Victoria3086, Australia, [2]Early Origins of Adult Health Research Group, Sansom Institute, University of South Australia, Adelaide, SA 5001, Australia and [3]Discipline of Physiology, University of Adelaide, Adelaide, SA 5005, Australia.

During development, the fetal heart undergoes a progressive increase in the ability to produce force related to evolving function. Developmental changes in some regulatory proteins of the cardiac contractile apparatus have been shown with gestational age. The troponin I molecule (Kruger *et al.,* 2006) has been examined in relation to birth with no attention to troponin T or C, major determinants of force development. Our understanding of the developmental changes in expression of various Troponin molecules is complicated by the fact that many studies are carried out in mammalian species, particularly in rats and mice, which undergo cardiomyocyte maturation after birth whereas this occurs in late gestation in humans and sheep. The aim of this study was to determine the expression of each of the major troponin molecules, T, I and C during late gestation fetal heart development.

All procedures were approved by the University of South Australia's animal ethics committee. At 110-125 days (d) gestation, surgery was performed in 13 pregnant ewes under aseptic conditions and general anesthesia. Vascular catheters were inserted as previously described in the maternal jugular vein, the fetal femoral and carotid arteries, jugular vein, and the amniotic cavity (Morrison et al., 2007). Fetal carotid arterial blood gas samples (0.5 ml) were collected daily for the measurement of fetal blood gases. At a range of gestational ages (110-140 d; term, 150 d), ewes (n = 23) were humanely killed with an overdose of sodium pentobarbitone (Lethobarb, 25 ml; 325 mg/ml) and fetuses were delivered by hysterotomy and weighed. The apex of the left ventricle was flash frozen in liquid nitrogen and stored at -80°C. The heart was reverse perfused with collagenase and protease to isolate cardiomyocytes which were fixed in 2% paraformaldehyde to allow for measurement of cardiomyocyte size and the percent of mononucleated cardiomyocytes. Western blots were performed on heart tissue using the Invitrogen NuPage Bis-Tris electrophoresis system. Primary antibodies for cardiac isoforms of Troponins C, T and I (Abcam Inc, Cambridge USA) were diluted 1:5000 and incubated on blots overnight at 4°C. Membranes were then incubated with a horse anti-mouse HRP conjugated secondary antibody at 1:2000 for 1hour (24°C), and bands visualized using ECL. Band densities were calculated using Quantity One software relative to internal controls.

Despite a decline in the percentage of mononucleated cardiomyocytes with increasing gestational age, there was no change in the expression of either troponin T or I. There was also no significant correlation between troponin T and I with either fetal weight, percent of left ventricular mononucleated cardiomyocytes (LVMC) or the size of left ventricular binucleated cardiomyocytes (LVBC). Troponin C, however, showed a 40% increase in protein expression ($p < 0.04$) after 120 d gestation. Furthermore, this increase in troponin C was positively correlated with both gestational age and fetal weight ($p < 0.04$). The percentage of mononucleated cardiomyocytes in the left ventricle was negatively correlated with troponin C protein expression.

These data show that changes in troponin C occur in late gestation tracking the timing of cardiomyocyte maturation. This may be the mechanism that supports our previous data showing little change in cardiac muscle contractility from 125 to 140 d gestation (Spencer *et al.,* 2006). Cardiomyocytes undergo binucleation after 110 d gestation in the sheep fetus (Burrell *et al.,* 2003) and this transition from mononucleated to binucleated cardiomyocytes may well be related to increased Troponin C expression and thus an increased ability to generate force.

Kruger M, Kohl T, Linke WA. (2006) *American Journal of Physiology* **291:** H496-506.

Morrison JL, Botting KJ, Dyer JL, Williams SJ, Thornburg KL, McMillen IC. (2007) *American Journal of Physiology*, **293:** R306-313.

Spencer TN, Botting KJ, Morrison JL, Posterino GS. (2006) *Journal Apply Physiology, **101:** 728-33,*

Burrell JH, Boyn AM, Kumarasamy V, Hsieh A, Head SI, Lumbers ER. (2003) Anatomical Record, **274A:** 952-61.

Characterisation of Suppressor of Cytokine Signalling protein expression in regenerating mouse skeletal muscle after injury

J. Stratton, K.T. Murphy, C. van der Poel and G.S. Lynch, Basic & Clinical Myology Laboratory, Department of Physiology, The University of Melbourne, VIC 3010, Australia.

Muscle injury can result in a significant loss of function that can impact on quality of life. A better understanding of the signalling pathways controlling skeletal muscle is critical for devising therapies to enhance muscle regeneration and function after injury. One of the key regulators of skeletal muscle regeneration is the JAK/STAT (Janus kinase/hyperlink) pathway, which transduces the signal of cytokines and growth factors. This pathway is negatively regulated by the Suppressor of Cytokine Signalling (SOCS) family of proteins. In many tissues, SOCS regulate inflammation, proliferation, differentiation and growth; important events for successful muscle regeneration. The expression patterns and relative importance of SOCS proteins during muscle regeneration have yet to be properly characterised. The aim of this study was to characterise SOCS1, SOCS2 and SOCS3 mRNA expression during skeletal muscle regeneration after injury, and examine the expression of Leukemia Inhibitory Factor (LIF), a key growth factor regulating SOCS expression.

Male C57BL/6 mice (˜12 weeks old) were anaesthetised deeply (76 mg/kg Ketamine and 10 mg/kg Xylazine; *i.p.*) and the tibialis anterior (TA) muscle injected with the myotoxin Notexin (1.6 mg/kg). Muscle function was assessed *in situ* at 7 days (n = 8), 14 days (n = 8) and 21 days (n = 7) post-injury using methods described in detail elsewhere (Schertzer *et al.*, 2007). Before performing functional analysis mice were anaesthetised (60 mg/kg Sodium pentobarbitone; *i.p.*). SOCS1, SOCS2, SOCS3 and LIF mRNA expression were assessed using Real-Time RT-PCR and normalised against total cDNA content.

Specific (normalised) force of injured TA muscles was decreased by 31%, 60% and 79% of control uninjured values at 7, 14 and 21 days, respectively ($p < 0.001$). Fibre cross-sectional area in injured muscles was 52% and 70% of control uninjured values at 7 and 14 days, respectively ($p < 0.05$). increased The percentage of centrally nucleated fibres was increased in injured muscles by 15-, 7- and 5-fold of control uninjured values at 7, 14 and 21 days, respectively ($p < 0.001$). SOCS2 mRNA expression was 30% lower at 7 days post-injury compared with uninjured controls ($p < 0.05$), but recovered to control uninjured levels by 21 days post-injury. There was no effect of injury on SOCS1 or SOCS3 mRNA expression at any time after injury. LIF mRNA expression was 400% higher at 21 days-post injury compared with control uninjured values ($p < 0.01$).

These preliminary findings implicate SOCS2 and LIF in successful muscle regeneration since they appear to play important regulatory roles in the events controlling muscle repair after injury.

Schertzer JD, Gehrig SM, Ryall JG, Lynch GS. (2007) *American Journal of Pathology*, **171:** 1180-8.
Spangenburg EE. (2007) *Exercise and Sports Science Reviews*, **35:** 156-62.

Supported by research grant funding from the Australian Research Council Discovery Project funding scheme (DP0665071; DP077281)

The effects of arsenic of the Na^+/K^+ ATPase transporter in the gills of the freshwater crayfish, *Cherax destructor*

Y. Lankadeva, G. Williams and J.M. West, School of Life and Environmental Sciences, Deakin University, 221 Burwood Hwy, Burwood, VIC 3125, Australia.

Arsenic is a ubiquitous element found in varying concentrations throughout the environment. It is a known carcinogen found at high concentrations in association with gold and other metals. Several anthropogenic activities, such as mining and agriculture can lead to elevated arsenic concentrations in the environment. Arsenic is found in the environment mainly as inorganic arsenic, arsenite (As(III)) and arsenate (As(V)) which are the most toxic and bioaccessible arsenic compounds.

Contamination in the environment can often lead to high levels of arsenic in surrounding water bodies. Thus aquatic animals are more highly exposed and affected than terrestrial animals as they are immersed in this toxin. Exposure to metal contamination has been shown to affect the function of a number of organs in a range of aquatic animals. Marine species are generally found to be more highly affected by metal exposure; however effects of metal contamination can vary amongst freshwater species.

The freshwater crayfish, *Cherax destructor* (Decapoda, Parastacidea) (yabbies), is the most widespread genus of Australian crayfish. Yabbies can accumulate significant amounts of arsenic within their tissues (Williams *et al*., 2008) and exposure to arsenic in their water results in reduced appetite and increased mortality post-moult.

This study aims to investigate the effects of arsenic exposure on the activity of the Na^+/K^+-ATPase transporter responsible for actively pumping sodium ions from the gill epithelium in yabbies exposed to 3ppm As(V) or As(III) in their water. Three gill filaments are attached to each walking leg. The three gill filaments on each of the four walking legs were used in the analysis. The activity of the Na^+/K^+ATPase transporter was measured using the method of McCormick & Bern (1989). The activity of this transporter was significantly different between the gill branches with the largest filament (22.3 nmol·mg $prot^{-1}·h^{-1}$) showing the highest activity in animals from the intermoult (8.3 nmol·mg $prot^{-1}·h^{-1}$ smallest gill). Activity was also significantly higher ($p < 0.05$) at different stages of the moult cycle in control animals (40.0 nmol·mg $prot^{-1}·h^{-1}$ – postmoult; 22.2 nmol·mg $prot^{-1}·h^{-1}$ - intermoult). Exposure to As(III) caused a significant reduction in transporter activity, but only after 12 weeks exposure from 40.0 nmol·mg $prot^{-1}·h^{-1}$ in the control animals to 17.4 nmol·mg $prot^{-1}·h^{-1}$ in the As(III) exposed animals (see Figure).

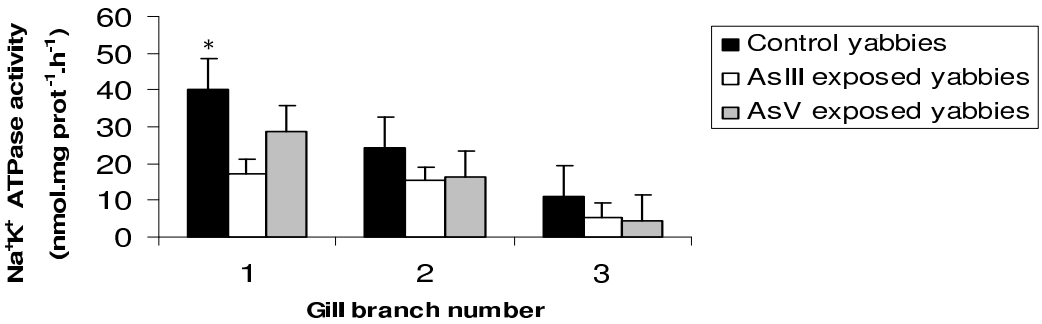

These results may explain the increased mortality seen in post-moult animals exposed to arsenite in their water. As new gill epithelium is laid down during the premoult, arsenic may alter the tissue structure such that their is reduced number of transporters or the level of activity of the Na^+/K^+-ATPase enzyme within the transporter is affected.

McCormick SD, Bern HA (1989) *American Journal of Physiology - Regulatory, Integrative and Comparative Physiology* **256**: 707-715.

Williams G, West JM, Snow ET (2008) *Environmental Toxicology and Chemistry* **27**:1332-1342.

Characterization of the muscle fibres types in a pristine and regenerate chela from the Christmas Island Red Crab *Geocarcoidea natalis*

J. Van Gramberg, S. Linton and J.M. West, School of Life and Environmental Sciences, Deakin University, 221 Burwood Hwy Burwood Victoria 3125, Australia.

This study investigated the relationship between chelae morphology and muscle fibre composition of the Christmas Island Red crab. Males of this species grow larger and develop asymmetrical chelae; females however possess smaller symmetrical chelae. This species is purely terrestrial and use their chelae for various functions including, burrowing, defense, courtship, grooming and walking.

Crustacean muscle fibres show great variation in fibre type which can be categorized by their greatly different sarcomere length (SL). Short-sarcomere fibres have a SL ≤ 4μm, a fast contraction speed, but produce relatively low forces. Fibres with long-sarcomeres have a SL > 6μm, exhibit a slower speed of contraction and develop considerably more force than short-sarcomere fibres (Atwood, 1976; West & Stephenson, 1993). Fibre types in crustaceans can also be distinguished by the contractile and regulatory protein isoforms they contain (Mykles, 1988; Koenders *et al*., 2004). Short-sarcomeres can be distinguished from long-sarcomere fibres by the presence of P75 (only expressed in fibres with short sarcomeres); the isoforms of paramyosin (short-sarcomere P1; long-sarcomere P2) and in the troponin I and T isoforms (Koenders *et al*., 2004).

Muscle fibre composition was determined in two morphologically distinct chelae types from male Red crabs. The large chela (propus and dactyl make contact only at the tips when chela is closed) and a regenerating chela (propus and dactyl have several points of contact when chela is closed). Chelipeds were removed at the basi-ischial joint, minimizing blood loss. Chelae were removed and thoroughly perfused with either 10% neutral buffered formalin or 70% ethanol. Fixed muscle fibres were dissected from specific regions in the lateral-interior surface of the pristine and regenerate chelae. SL of fibres was determined using a He-Ne laser and confirmed using histology. Protein isoforms of several fibres with greatly different sarcomere length were separated using SDS-PAGE.

72% of male crabs had the large chelae on the left hand side. A total of 766 fibres were dissected from 11 different areas of the pristine chela and 870 fibres from 9 areas in the regenerating chela and their SL determined. Fibres in both chelae exhibited a broad range of SL's ranging from 3-21μm (pristine) and 3-15 μm (regenerate). The average SL of fibres was 9.66μm and 8.45μm in the pristine and regenerate chelae respectively. The number of fibres with a SL < 4μm was one in the pristine and twelve in the regenerate indicating that only a very small number of fast contracting fibres are present. Regenerate chela in other crustacean species, have a greater proportion of fibres with short-sarcomeres in the central portions of the chela. No such trend was observed in the Red crab. Fibres from the chelae with a sarcomere length just under 4μm do not express the proteins characteristically used to identify short-sarcomere fibres, namely P75. Thus the fibres in the chelae of the Christmas Island Red crab suggest a continuum in fibre type with the majority of fibres expressing proteins of the long-sarcomere fibre type but having a broad range of sarcomere lengths.

Atwood, H.L (1973) *American Zoologist* **13**: 357-378.

Koenders, A., Lamey, T.M., Medler, S., West, J.M. & Mykles, D.L (2004) *Journal of Experimental Zoology Part A: Comparative Experimental Biology*, **301A**: 588-598.

Mykles, D.L (1988) *Journal of Experimental Zoology*, **245**: 232-243.

West, J.M. & Stephenson, D.G.(1993) *Journal of Physiology*, **462**: 579-596.

Comparison of contractile characteristics of permeabilized muscle fibres from the golden retriever muscular dystrophy (GRMD) dog and the *mdx* dystrophic mouse

H.Q. Lim,[1] C. van der Poel,[1] J.E. Church,[1] J.C.S. Bizario,[2] M.C.R. Costa,[2] M.L. Pinto[2] and G.S. Lynch,[1] [1]Basic and Clinical Myology Laboratory, Department of Physiology, The University of Melbourne, VIC 3010, Australia and [2]Associação de Amigos dos Portadores de Distrofia Muscular, University of Ribeirão Preto, São Paulo, Brasil.

Duchenne muscular dystrophy (DMD) is a severe X-linked progressive muscle disease caused by the absence of dystrophin. A number of animal models are available to investigate underlying mechanisms and identify potential therapies for DMD. Although the most commonly used animal model of DMD, the *mdx* mouse, carries the same genetic mutation of the dystrophin gene, it exhibits a considerably milder phenotype (Lynch, 2004). The golden retriever muscular dystrophy (GRMD) dog represents an appealing animal model for DMD as it not only shares the mutation in the dystrophin gene but also exhibits a similar phenotype (Childers *et al*. 2002). Few GRMD dog colonies exist worldwide, making it a unique but not widely used model. Little information exists about many of the fundamental aspects of skeletal muscles from dystrophic compared with healthy dogs. The aim was to identify Ca^{2+}- and Sr^{2+}-activated contractile characteristics of single muscle fibres from dystrophic dogs and to compare these with fibres from *mdx* dystrophic mice.

GRMD dogs (n = 3) and littermate controls (n = 3) were housed in the University of Ribeirâo Preto Sao Paulo, Brazil. Dogs were anaesthetized (Tiletamine Cloridrate 125.0 mg and Zolazepam Cloridrate 125.0 mg) and open muscle biopsies taken from the biceps femoris muscle. All dogs recovered from the anaesthesia. The muscle samples were tied to a capillary tube and placed immediately in a vial containing skinning solution of the following composition (mM): potassium propionate, (125), EGTA (5), ATP (2), $MgCl_2$ (2), imidazole, 20; and 50 % v/v glycerol, adjusted to pH 7·1 with 4 M KOH; and stored at -20°C for up to 12 weeks (Lynch *et al.* 2000). C57BL/10 and *mdx* mice were killed by cardiac excision while anaesthetized (sodium pentobarbital, 60 mg/kg, *i.p.*) and the extensor digitorum longus (EDL) and soleus muscles were surgically excised and immersed in skinning solution for preparation of permeabilized muscle fibres. Individual fibres were isolated, attached to a sensitive force recording device, and immersed in a series of solutions with increasing $[Ca^{2+}]$ and $[Sr^{2+}]$. After the contractile properties had been determined, the fibre segments were stored for later analysis of contractile and regulatory protein isoforms by SDS-PAGE.

There was a significant decrease in maximum Ca^{2+}-induced force by GRMD dog fibres (120 ± 1 kN/m^2, n = 62), compared with littermate controls (134 ± 2 kN/m^2, n = 67), however, maximum Ca^{2+}-induced force was not different between EDL or soleus muscle fibres from *mdx* and C57BL/10 mice. There was a significant decrease in the Hill coefficient (n_H) of the force-pCa relationship for GRMD dogs, compared with littermate controls but n_H was not different between fibres from *mdx* and C57BL/10 mice. Fibre sensitivity to Ca^{2+} (pCa_{50}) was not different between GRMD dogs (5.95 ± 0.02, n = 55) and littermate controls (5.99 ± 0.03, n = 54) nor was it different between *mdx* and WT mice. These findings highlight differences between animal models for DMD and that a lack of dystrophin can result in variable phenotypes between species.

Childers MK, Okamura CS, Bogan DJ, Bogan JR, Petroski GF, McDonald K, Kornegay JN. (2002). *Archives of Physical Medicine and Rehabilitation* , **83:** 1572-8.

Lynch GS. (2004). *Clinical and Experimental Pharmacology and Physiology*, **31:** 557-61.

Lynch GS, Rafael JA, Chamberlain JS, Faulkner JA. (2000) *American Journal of Physiology*, **279:** C1290-4.

Supported by the Muscular Dystrophy Association (USA)

The location of nascent proteins in mechanically skinned skeletal muscle fibres of the rat

D.W. Jame,[1] M. Jois,[2] M. McDonagh[3] and D.G. Stephenson,[1] [1]Department of Zoology, La Trobe University, VIC 3086, Australia, [2]School of Life Sciences, La Trobe University, VIC 3086, Australia and [3]Victorian Department of Primary Industries, Attwood, VIC 3049, Australia.

A novel technique for measuring protein synthesis in segments of single mechanically skinned muscle fibres was recently developed by us to investigate the cellular and molecular events underpinning protein synthesis in muscle (Jame, Jois & Stephenson, 2006 & 2007). Given the absence of a surface membrane, which is removed in this preparation by microdissection, it was important to determine where in the preparation the newly synthesised proteins are located.

As previously described, mechanically skinned fibre segments were prepared from freshly dissected soleus muscles of rats (3-5 months old Long-Evans, hooded) killed by isoflurane overdose in accordance with animal ethics procedures approved at La Trobe University. The skinned fibre segments were then incubated at 30^{o}C for 2 hours in a medium mimicking the myoplasmic ionic environment and containing ^{3}H-leucine and a mixture of all the 20 amino-acids required for protein synthesis (Jame, Jois & Stephenson, 2007). Protein synthesis was determined by measuring the difference between ^{3}H-leucine incorporation in paired segments of the same skinned fibre, one incubated in the absence and the other in the presence of the well established protein synthesis inhibitor, cycloheximide (CHX). Following incubation, the two fibre segments were washed under identical conditions and then the membranous compartments of the single skinned muscle fibre segments were lysed by osmotic shock, in double distilled H_2O followed by freezing and thawing and finally by exposure to 1% Triton X-100 in a relaxing solution heavily buffered for very low free [Ca^{2+}].

Effectively all CHX-sensitive ^{3}H-leucine incorporation in the mechanically skinned fibres could be released when the intracellular membrane compartments were subjected to the lysing procedure (103 ± 30 % total CHX-sensitive ^{3}H-leucine incorporation, n = 7), indicating that the newly synthesised proteins were accumulating in a membraneous compartment. As any protein synthesis occurring on free ribosomes would be expected to freely diffuse out in the absence of a surface membrane, the results provide strong evidence that the major site for protein synthesis measured in the skinned fibre preparation is the rough endoplasmic (sarcoplasmic) reticulum. Considering that the sarcoplasmic reticulum remains structurally and functionally intact after the skinning procedure (Lamb, Junankar & Stephenson, 1995), this study shows that it is now possible to measure protein synthesis at single muscle fibre level associated with the intact rough endoplasmic (sarcoplasmic) reticulum under controlled conditions.

Jame DW, Jois M, Stephenson DG. (2006) *Proceedings of the Australian Physiological Society*, **37**: 62P.
Jame DW, Jois M, Stephenson DG. (2007) *Proceedings of the Australian Physiological Society*, **38**: 107P.
Lamb GD, Junankar PR, Stephenson DG. (1995) *Journal of Physiology*, **489**: 349-362.

This study was supported by an NH&MRC grant.

The effect of taurine supplementation on taurine transporter content and ROS-induced lipid peroxidation during fatiguing contractions in rat skeletal muscle

C.A. Goodman,[1,2,4] D. Horvath,[3,4] C.G. Stathis,[3,4] K. Croft[5] and A. Hayes,[3,4] [1]School of Human Movement, Recreation and Performance, Victoria University, Melbourne, VIC 8001, Australia., [2]Department of Physiology, The University of Melbourne, Parkville, VIC 3010, Australia, [3]School of Biomedical and Health Sciences, Victoria University, Melbourne, VIC 8001, Australia, [4]Centre for Ageing, Rehabilitation, Exercise and Sport, Victoria University, Melbourne, VIC 8001, Australia and [5]School of Medicine and Pharmacology, University of Western Australia, Crawley, WA 6009, Australia.

Taurine (Tau; 2-aminoethane sulfonic acid), a non-toxic beta amino acid found in most mammalian cells, is reported to function as an osmotic regulator, a cell membrane stabilizer, a modulator of inflammation, an intracellular ion regulator (esp. calcium) and a direct or indirect antioxidant (for review see Huxtable, 1992). Studies in liver have shown that Tau may attenuate non-enzymatic reactive oxygen species (ROS)-induced lipid peroxidation (e.g. Yildirim *et al.*, 2007). It has also been shown in various cell lines and tissues that increased Tau levels down-regulates Tau transporter mRNA and protein expression (Tappaz, 2004). The aim of this study was to investigate: 1) whether Tau supplementation would increase muscle Tau content and lead to a decrease in Tau transporter protein; 2) whether continuous or repeated fatiguing tetanic contractions would lead to an increase in non-enzymatic ROS-induced lipid peroxidation as indicated by F_2-isoprostane production; and 3) whether increased muscle Tau can reduce any non-enzymatic ROS-induced lipid peroxidation during fatiguing repeated tetanic contractions.

Male Sprague Dawlay rats (8 wks) were supplemented with Tau in drinking water (2.5% w/v) for 2 weeks. Fast twitch *extensor digitorum longus* (EDL) muscles were dissected out under anaesthesia (Nembutal; 85mg/kg) in accordance with Victoria University AEEC procedures and subjected to one of two different stimulation protocols: 1) 10s continuous stimulation at a frequency of 100Hz (0.2ms pulse duration); 2) 3 min intermittent stimulation (1s stimulation at 100Hz followed by 4s recovery). Fatigued muscles and their non-fatigued contra-lateral controls were blotted, weighed, frozen in liquid N_2 and F_2-isoprostanes analysed by GC/MS (Mori *et al.*, 1999). Non-fatigued control muscles were also analysed for Tau content by HPLC and Tau transporter protein by western blotting.

Tau supplementation increased muscle Tau content by 39.5% (p = 0.0002, n=8) with no change in Tau transporter protein (p = 0.41, n=8). Ten seconds of continuous fatiguing tetanic stimulation, which reduced tetanic force by 60-66% of initial force, did not result in a change in the level of F_2-isoprostanes in either non-supplemented (n=8) or Tau supplemented muscles (n = 8) compared to their non-stimulated contra-lateral controls. After 3 min of intermittent stimulation, however, in which tetanic force was reduced by 90-92%, there was a significant main effect (p=0.0003; 2-way ANOVA with Bonferoni post-test) for contractions to increase F2-isoprostane levels by 46.7% (1.47 ± 0.09 *vs* 2.16 ± 0.13 pg F_2-isoprostanes/μg arachidonic acid; n = 8) and by 13.0 % (1.85 ± 0.13 *vs* 2.09 ± 0.09 pg F_2-isoprostanes/μg arachidonic acid; n = 8) compared to non-stimulated contra-lateral control muscles (n = 8). There was also a strong trend (p = 0.06) for Tau to attenuate F_2-isoprostane production than stimulated control muscles.

In conclusion, 2 wks of Tau supplementation significantly increased muscle Tau content but did not cause a down-regulation of Tau transporter protein expression. In addition, repeated tetanic contractions led to a significant increase in non-enzymatic ROS-induced lipid peroxidation, as indicated by raised F_2-isoprostane content. There was a strong trend for Tau to attenuate lipid peroxidation.

Huxtable RJ (1992) *Physiolgical Reviews*, **72**, 101-163.
Mori TA, Croft KD, Puddey IB, Beilin LJ. (1999) *Analytical Biochemistry*, **268**, 117-127.
Tappaz ML (2004) *Neurochemistry Research*, **29**, 83-96.
Yildirim Z, Kiliç N, Ozer C, Babul A, Take G, Erdogan D. (2007) *Annals of the New York Academy of Science*, **1100**, 553-561.

Stretch-induced force enhancement in fast and slow skeletal muscle: implications for damage and disease

K.A. Ramsey, G.J. Pinniger and A.J. Bakker, Discipline of Physiology, School of Biomedical, Biomolecular and Chemical Sciences, University of Western Australia, Crawley, WA 6009, Australia.

When an actively contracting skeletal muscle is stretched, the force it exerts increases throughout the stretch due to the strain of contractile and non-contractile proteins (Edman, Elzinga & Noble, 1978). After the stretch this force enhancement decays to a new steady-state force, which is higher than the isometric force at the corresponding length, often referred to as residual force enhancement (RFE). The mechanism of RFE is still unknown, although previous studies suggest it may be caused by the strain of activated non-contractile proteins, such as titin (Pinniger, Ranatunga & Offer, 2006). In order to evaluate the possible role of titin in stretch-induced force enhancement we compared the force enhancement characteristics in fast (EDL) and slow (SOL) muscle, known to differ in their titin isoforms (Wang *et al.*, 1991).

EDL and SOL muscles were removed from the hindlimb of adult male Wistar rats under deep anesthesia (IP sodium pentobarbitone, 40 mg/kg) and mounted in an *in vitro* muscle test system (1200A; Aurora Scientific, Aurora, Canada) containing mammalian Ringer solutions bubbled with 90% O_2 / 5% CO_2 at 25 °C. We examined the stretch-induced force response by applying a series of small amplitude stretches (5% optimal fibre length, L_0) to the plateau of an isometric contraction at a range of constant velocities (0.1-10 $L_0.s^{-1}$). Based on the force-velocity profile we quantified the velocity-dependent contractile and velocity-independent non-contractile contributions to force enhancement during stretch, and RFE after stretch in EDL and SOL muscles (Pinniger, Ranatunga & Offer, 2006).

RFE was significantly higher in EDL than SOL ($p < 0.01$; see figure). This supports our hypothesis that the non-contractile contribution to force enhancement is higher in fast muscle and maybe due to a shorter, stiffer titin filament. We also examined the non-contractile contributions to stretch-induced force enhancement in damaged and dystrophic muscle. Following a series of 10 damaging eccentric contractions (20% L_0) RFE increased significantly (3-4 times) in both EDL and SOL ($n = 9$, $p < 0.01$), which suggests that non-contractile proteins may be overstretched as a result of muscle damage. Furthermore, RFE was significantly lower in dystrophic muscles from *mdx* mice compared to non-dystrophic control (C57BL/10) mice in EDL (mdx 0.03 ± 0.005 P_o ($n = 4$), control 0.06 ± 0.004 P_o ($n = 4$), $p < 0.01$) and SOL (mdx ($n = 4$) 0.02 ± 0.002 P_o, control 0.03 ± 0.003 P_o ($n = 4$, $p < 0.01$) muscles.

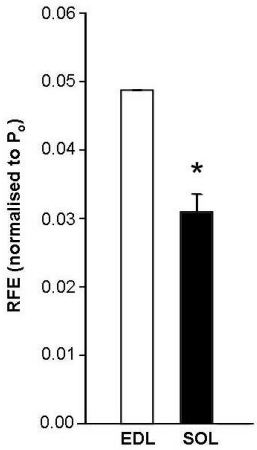

The results of this study are consistent with the hypothesis that titin plays a significant role in stretch-induced force enhancement. Titin is ideally situated within the sarcomere to act as a sensor for mechanical strain that may, via complex interactions with other sarcomeric proteins, be crucial for the activation of various signalling pathways associated with muscle development and adaptation. Based on the changes observed in the magnitude of RFE we propose that the activation of these pathways may be enhanced after muscle damage and impaired in diseased muscle, *e.g.*, Duchenne muscular dystrophy.

Edman K., Elzinga G & Noble M. (1978) *Journal of Physiology*, **281:** 139-55.
Pinniger G, Ranatunga K & Offer G. (2006) *Journal of Physiology* **573:** 627-43.
Wang K, McCarter R, Wright J, Beverly J & Ramirez-Mitchell R. (1991) *Proceedings of the National Academy of Sciences USA*, **88:** 7101-5.

Age-related alterations in transforming growth factor-β (TGF-β) signalling in rat skeletal muscle: implications for sarcopenia

K.T. Murphy, J.G. Ryall, R. Koopman and G.S. Lynch, Basic and Clinical Myology Laboratory, Department of Physiology, The University of Melbourne, VIC 3010, Australia.

Ageing is associated with a progressive loss of muscle mass (sarcopenia) and strength. With Australia's demographic shifting towards an older population, and ageing already contributing significantly to our health care costs, sarcopenia is a major public health concern. Myostatin, a member of the transforming growth factor-β (TGF-β) superfamily, is a negative regulator of muscle mass and an age-related increase in myostatin expression (Léger *et al.,* 2008) is thought to contribute to sarcopenia. Whether the intracellular Smad signalling pathway tranducing the myostatin signal (and other TGF-β ligands) is altered with ageing is unknown. We tested the hypothesis that the protein abundance of Smad3 and Smad4, intracellular mediators of TGF-β signalling that translocate to the nucleus to suppress the transcription of muscle regulatory factors such as MyoD and myogenin, would be elevated in muscles aged; whereas protein abundance of Smad7, an inhibitory molecule that prevents the phosphorylation and nuclear translocation of Smad3/4, would be lower in muscles from aged compared with young rats.

Young (3 month, n = 5), adult (16 month, n = 5) and old (27 month, n = 5) F344 rats (Ryall *et al.*, 2007) were anaesthetised deeply (60 mg/kg sodium pentobarbitone, *i.p.*) and tibialis anterior (TA) muscles excised and analysed for the protein abundance (western blotting) of Smad3, Smad4 and Smad7.

TA muscles from adult and old rats had higher Smad3 protein abundance (by ~300 and ~400%, respectively) compared with young rats (the Figure). TA muscles of old rats also had lower Smad7 protein abundance (by ~80%), compared with young rats (the Figure). There was no difference in Smad4 protein abundance between age groups.

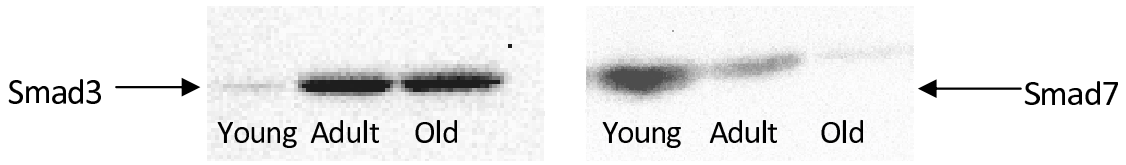

The findings raise important questions as to whether ageing is associated with alterations in the localisation of Smad3 and Smad7, and whether the lower Smad7 protein abundance in the TA of old rats involves: i) reduced Smad7 acetylation; ii) increased association with histone deactyalase 1 (HDAC1), resulting in Smad7 deactylation; or iii) increased association with Smurf1, leading to Smad7 ubiquination.

This study revealed that in rats, ageing is associated with an enhanced Smad3 protein abundance and a corresponding reduction in protein abundance of the inhibitory Smad7. These findings implicate increased TGF-β superfamily signalling in the negative regulation of muscle mass and ultimately, to age-related muscle wasting and weakness. A better understanding of the cellular mechanisms underlying sarcopenia may lead to potential therapeutic strategies to attenuate sarcopenia.

Léger B, Derave W, De Bock K, Hespel P, Russell AP. (2008) *Rejuvination Research*, **11:** 163-175B.
Ryall JG, Schertzer JD, Lynch GS. (2007) *Journal of Gerontology: Biological Sciences*, **62:** 813-23.

Supported by research grant funding from the Australian Research Council Discovery Project funding scheme (DP0665071; DP077281) and Pfizer Inc. (USA).

Twitch kinetics of adult and aged EDL muscle from an α-actinin-3 knockout mouse

S. Chan,[1] S.I. Head[1] and K.N. North,[2] [1]Department of Physiology, University of New South Wales, NSW 2052, Australia and [2]Children's Hospital at Westmead, Neurogenetics Research Unit, Westmead, NSW 2145, Australia.

The actin-binding protein α-actinin-3 is specifically expressed in fast glycolytic muscle fibres. Homozygosity for a common polymorphism in the ACTN3 gene results in complete deficiency of α-actinin-3 in about 16% of individuals worldwide. Although α-actinin-3 deficiency does not cause disease in α-actinin-3 knockout mice, recent studies suggest that the absence of α-actinin-3 is detrimental to sprint and power performance in elite athletes (Yang *et al.*, 2003). Recent studies also suggest that in young mice there is an alteration in the metabolic profile of the fast muscle such that fast-twitch, glycolytic fibres have slower-twitch, more oxidative properties without an alteration in the overall expression of myosin 2B. To determine the effect of α-actinin-3 deficiency on the twitch kinetics of whole skeletal muscle, we studied isolated extensor digitorum longus (EDL) muscles from α-actinin-3 knockout mice and wild-type littermate controls. Animals were examined in 2 age groups: "Adult" (8 weeks to 6 months) and "Aged" (20 to 22 months).

Animals were sacrificed with an overdose of halothane (ethics approval UNSW). The EDL muscle was dissected from the hindlimb and tied by its tendons to a force transducer at one end and a linear tissue puller at the other. It was placed in a bath continuously superfused with Krebs solution, with composition (mM): 4.75 KCl, 118 NaCl, 1.18 KH_2PO_4, 1.18 $MgSO_4$, 24.8 $NaHCO_3$, 2.5 $CaCl_2$ and 10 glucose, with 0.1% fetal calf serum and continuously bubbled with 95% O_2-5% CO_2 to maintain pH at 7.4. The muscle was stimulated by delivering a supramaximal current between two parallel platinum electrodes. At the start of the experiment, the muscle was set to the optimum length L_0 that produced maximum twitch force. All experiments were conducted at room temperature (~22°C to 24°C). Muscles were subjected to fatiguing stimulation consisting of one-second, 100-Hz stimuli given every 2 seconds over a period of 30 seconds. Twitches were recorded both before and immediately after this fatigue protocol, and twitch half-relaxation times were measured from these recordings.

Before fatigue, the half-relaxation times of knockout (KO) muscles were not significantly different from wild-types (WT) in either age group. However, following the fatigue protocol, the half-relaxation times of knockouts were significantly higher than those of wild-type muscles, and this difference was more pronounced in the younger ("adult") age group. In the younger ("adult") age group, there was a 6.2 ms difference (20.5 ± 0.8 ms, n=13 for KO *versus* 14.3 ± 0.6 ms, n=12 for WT, $p < 0.001$) while in older ("aged") animals there was a 2.8 ms difference (17.0 ± 0.9 ms, n=10 for KO *versus* 14.2 ± 0.5 ms, n=11 for WT, $p < 0.05$).

These data suggest that in fatigued muscles, α-actinin-3 deficiency is associated with longer half-relaxation times and this lengthening is more pronounced in younger animals. This increase in half-relaxation time may be related to the observation that absence of α-actinin-3 is detrimental to sprinting performance in elite athletes.

Yang, N, MacArthur, DG, Gulbin, JP, Hahn, AG, Beggs, AH, Easteal, S & North, K. (2003). ACTN3 genotype is associated with human elite athletic performance. *American Journal of Human Genetics* **73,** 627-631

The effects of acute exercise and creatine supplementation on Akt signalling in human skeletal muscle

R.J. Snow, C.R. Wright, M.J. Quick, A.P. Garnham, K.K. Watt and A.P. Russell, The Centre for Physical Activity and Nutrition Research (C-PAN), School of Exercise and Nutrition Sciences, Deakin University, VIC 3125, Australia.

Introduction. The protein kinase Akt has recently been described as a major signalling pathway regulating skeletal muscle remodelling. Stimulation of the Akt signalling pathway through IGF/IRS/PI3K activates a series of downstream anabolic targets including Glycogen Synthase Kinase 3β (GSK-3β) and the mammalian target of rapamycin (mTOR) (Bodine *et al.*, 2001) and can also inhibit catabolic pathways involving Forkhead Transcription Factors (FOXO) and their atrophy gene targets, atrogin-1 and MuRF1 (Stitt *et al.*, 2004). It has recently been shown that Akt and GSK-3β phosphorylation is increased within a few hours following moderate intensity endurance exercise (Mascher *et al.*, 2007). However, whether endurance exercise regulates other Akt targets such as mTOR or FOXO was not determined. Creatine supplementation is also associated with increases in IGF-1 mRNA (Louis *et al.*, 2004) and by analogy, could also increase the phosphorylation and activation of Akt. It is therefore possible that both endurance exercise and creatine supplementation could stimulate Akt and its downstream pathways. At present the effect of endurance exercise and creatine supplementation on the phosphorylation of Akt and its downstream signalling targets has not been investigated in humans. The aim of this study was to determine the effects of acute endurance exercise, with/and without creatine supplementation, on the phosphorylation status of proteins involved in the Akt signalling pathways; Akt/GSK-3β, Akt/mTOR, Akt/FOXO.

Methods. Sixteen healthy male subjects performed single leg cycling at 65% VO2 peak until exhaustion. Subjects were randomly assigned to a creatine or placebo group and were administered either 0.4 g/kg of creatine monohydrate with 0.4 g/kg of glucose or 0.8 g/kg of glucose, respectively, for five days post exercise. Muscle biopsies were taken before the exercise bout and at 3 hours, 1 day and 5 days post exercise from both the exercising and non-exercising legs. Biopsies were taken for the non-exercising leg to control for the potential confounding effects of inflammation induced by multiple muscle biopsies. Cytosolic and nuclear proteins were separated and phosphorylation levels of Akt, GSK-3β, mTOR, 4EBP1, Foxo1 and Foxo3a were analyzed by western blotting. IGF-1 mRNA expression was measured using quantitative PCR.

Results. A 3-way ANOVA revealed a strong trend ($p = 0.067$) and a significant interaction ($p = 0.023$) between treatment (creatine *vs* placebo) x exercise x time for Akt and GSK3β phosphorylation levels, respectively. For Akt, further analyses demonstrated a trend ($p = 0.076$) for an interaction between treatment and time suggesting an increase in Akt phosphorylation levels at days 1 and 5 in the creatine group. Along similar lines, GSK3β phosphorylation levels were increased at days 1 and 5 in the creatine group. There was no interaction or main effects for mTOR, 4EBP1, Foxo1 and Foxo3a phosphorylation levels or IGF-1 mRNA.

Conclusion. These observations suggest that creatine supplementation for 1 to 5 days may increase the activity of the Akt/ GSK-3β signalling pathway. Acute single leg endurance exercise does not appear to affect the phosphorylation levels of Akt or its downstream signalling proteins, when measured 3 hours, 1 day and 5 days post exercise.

Bodine SC. Stitt TN, Gonzalez M, Kline WO, Stover, GL, Bauerlein R, Zlotchenko E, Scrimgeour A, Lawrence JC, Glass DJ & Yancopoulos GD. (2001) *Nature Cell Biology*, **3:** 1014-9.

Louis M, Van Beneden R, Dehoux M, Thissen JP & Francaux M. (2004) *FEBS Letters*, **557:** 243-7.

Mascher H, Andersson H, Nilsson PA, Ekblom B & Blomstrand E. (2007) *Acta Physiologica (Oxford)*, **191:** 67-75.

Stitt TN, Drujan D, Clarke BA, Panaro F, Timofeyva Y, Kline WO, Gonzalez M, Yancopoulos, GD & Glass DJ. (2004) *Molecular Cell*, **14:** 395-403.

Effects of exercise training and antioxidant supplementation on endothelial cell gene expression

A. Matsumoto,[1] L.C. Ward,[2] P.A. Wilce,[2] S.A. Marsh,[3] R.G. Fassett[4] and J.S. Coombes,[1] [1]School of Human Movement Studies, The University of Queensland, St Lucia QLD 4072, Australia, [2]School of Molecular & Microbial Science, The University of Queensland, St Lucia QLD 4072, Australia, [3]Department of Nutrition and Exercise Metabolism, Washington State University, PO Box 1495 Spokane WA 99210-1495, USA and [4]Royal Brisbane Women's Hospital, GPO Box 48, Brisbane QLD 4001, Australia.

Introduction. There are many studies to support that regular exercise is cardioprotective. It is established that exercise training has a beneficial effect on cardiovascular risk factors however these improvements do not explain all exercise-induced elements of cardioprotection. Additional molecular mechanisms by which exercise provides cardioprotection are poorly understood. Recent data suggests that exercise-induced alterations in myocardial and vascular endothelial cells may provide cardioprotection. Ras homolog gene family member A (RhoA) is a protein shown to regulate important cell functions, such as contraction, migration, proliferation, apoptosis and gene expression. Rho kinases (ROCKs) are the first downstream effector of RhoA, and studies have shown that RhoA/ROCK plays a significant role in arteriosclerotic disease as well as vascular smooth muscle cell hypercontraction. Specifically in endothelial cells, the RhoA/ROCK pathway induces endothelial dysfunction by decreasing the synthesis of the vasodilator, nitric oxide. This can also effect endothelial barrier disruption by increased permeability, enhance inflammation and atherothrombosis. These factors may explain the importance of this pathway in relation to cardiovascular disease. Little research has studied the effect of exercise on RhoA. The purpose of this study was to investigate the effects of exercise and/or antioxidant supplement on myocardial and vascular endothelium gene expression, specifically Ras homolog gene family member A.

Method. Male Wistar rats (N = 48) were divided into four groups: i) antioxidant; ii) exercise; iii) antioxidant and exercise; and iv) control. Exercise group underwent 14 weeks of endurance running on a motorised treadmill (90min/day, 4days/week, at 70% VO_2max). Animals in the supplement group received Vitamin E (1000 IU/kg diet) and α-lipoic acid (1.6g/kg diet) mixed with rat chow. After 14 weeks, rats were sacrificed and tissues were collected. Myocardial and coronary artery ECs were isolated from the hearts. The 27K rat genome oligo slides were used to conduct cDNA microarray analysis on those ECs.

Results. 2-Way ANOVA revealed that gene expression levels on 35, 40 and 40 were altered for the exercise, antioxidant supplementation and interaction of exercise and antioxidant supplementation respectively. Specifically, Ras homolog gene family member A (RhoA) was down-regulated by the effect of exercise ($P < 0.02$).

Conclusion. Inhibition of the RhoA/ROCK pathway might be one of the mechanisms to explain the positive effect of exercise on CVD. Future research on the effect of exercise on RhoA/ROCK may provide important information to further understand the molecular mechanism of exercise cardioprotection. Confirmation of these results by real-time RT-PCT and western blot will be conducted.

The effect of acute exercise on skeletal muscle SIRT1

S.E. Heywood, G.D. Wadley and G.K. McConell, Exercise Physiology and Metabolism Laboratory, Department of Physiology, The University of Melbourne, VIC 3010, Australia.

Introduction. Previous studies have shown acute exercise increases peroxisome proliferator-activated receptor γ coactivator-1α (PGC-1α) transcriptional activity, regulating contraction-induced mitochondrial biogenesis in skeletal muscle. Fasting in rodents and *in vitro* studies suggest SIRT1, a protein deacetylase allosterically activated by NAD^+, may stimulate this pathway in skeletal muscle through its deacetylation and activation of PGC-1α. Fasting, which elevates the cellular metabolic NAD^+:NADH ratio, increases SIRT1 expression and reduces PGC-1α acetylation in rodent skeletal muscle implying SIRT1 to be active in this metabolic profile. Whilst it has been assumed acute exercise stimulates this pathway through increases in the NAD^+:NADH ratio, no study has examined whether this SIRT1/PGC-1α interaction is activated by acute exercise. This experimental study examined the effect of acute exercise on SIRT1 activity, interaction of SIRT1 with PGC-1α, and mRNA and protein expression of SIRT1 and PGC-1α within rat skeletal muscle. As previous findings implicate SIRT1 to regulate skeletal muscle PGC-1α pathways during fasting, the fed state of the rats was controlled for.

Methods. Six-week old male Sprague-Dawley rats were randomly allocated to one of six groups (n=8 per group). Three groups were *ad libitum* fed, three groups were overnight fasted (16 hours). For each fed state one group of rats was killed at rest, one group was killed immediately following one hour of acute exercise on a motorized treadmill (25m/min at a 5% incline), and one group was killed three hours post acute exercise. Gastrocnemius muscle was rapidly excised, frozen in liquid nitrogen and used for all analyses.

Results. No change in SIRT1 activity was detected following fasting or exercise, implying that fasting and exercise did not cause covalent modification of SIRT1 and that allosteric binding of NAD^+ (which is lost during the extraction) may be the primary regulator of SIRT1 activity under these circumstances. Attempts to immunoprecipitate PGC-1α were unsuccessful, therefore we were unable to examine PGC-1α acetylation (as an indicator of SIRT1 activity *in vivo*). Immunoprecipitation for SIRT1 revealed PGC-1α to directly associate with SIRT1 in skeletal muscle, although exercise and fasting did not appear to alter the extent of this association. Three hours following acute exercise PGC-1α mRNA was significantly higher ($p < 0.05$). Fasting further increased PGC-1α mRNA expression three hours post acute exercise ($p < 0.05$), in parallel with a tendency for increased SIRT1mRNA expression ($p = 0.07$). However, exercise and fasting had no effect on PGC-1α or SIRT1α protein levels.

Conclusions. This study has demonstrated that SIRT1 and PGC-1α interact in skeletal muscle *in vivo*, and that SIRT1 mRNA has a tendency to increase following acute exercise in a fasted, but not fed state. Fasting increases PGC-1α mRNA expression following acute exercise to a greater extent than exercise in fed condition. Further investigation is required to investigate whether the SIRT1/PGC-1α interaction facilitates deacetylation during exercise *in vivo*.

Exercise-training increases skeletal muscle mitochondrial biogenesis despite inhibition of xanthine oxidase

M.A. Nicolas, G.K. McConell and G.D. Wadley, Department of Physiology, The University of Melbourne, Parkville, VIC 3010, Australia.

Reactive oxygen species (ROS) increase in skeletal muscle during exercise and there is some evidence that such small, physiological increases in ROS are required for normal increases in mitochondrial biogenesis following exercise (Gomez-Cabrera *et al.*, 2008). Indeed, vitamin C, a non-specific antioxidant, prevents increases in mitochondrial biogenesis markers during exercise-training in rats (Gomez-Cabrera *et al.*, 2008). Although several ROS producing sites have been identified in skeletal muscle during contraction, there is a lack of knowledge regarding the source(s) of ROS responsible for initiating pathways culminating in mitochondrial biogenesis in skeletal muscle during exercise. A recent study has identified the enzyme xanthine oxidase (XO) as a potential source of ROS responsible for initiating skeletal muscle mitochondrial biogenesis during exercise (Gomez-Cabrera *et al.*, 2005). p38 MAPK is a putative mitochondrial biogenesis signalling molecule (Akimoto *et al.*, 2005) and the inhibition of the XO-mediated ROS production during acute exercise *in vivo* with the XO inhibitor, allopurinol, prevented increases in gastrocnemius p38 MAPK phosphorylation immediately after exercise (Gomez-Cabrera *et al.*, 2005). However, key mitochondrial biogenesis proteins were not analysed and the effect of allopurinol during exercise-training has not been examined. Therefore the aim of this investigation was to determine whether inhibiting XO-induced increases in ROS with allopurinol during exercise training attenuates key proteins involved in mitochondrial biogenesis.

Male Sprague-Dawley rats aged 5 weeks were randomly assigned into four groups: [1] Sedentary (SedWater) (n=6); [2] Exercise-trained (ExWater) (n=6); [3] Sedentary and treated with 0.25 mg/mL of allopurinol in drinking water (SedAllo) (n=6); and [4] Exercise-trained and treated with 0.25 mg/mL of allopurinol in drinking water (ExAllo) (n=6). Pilot testing revealed this treatment to inhibit phosphorylation of p38 MAPK during acute exercise. Trained rats were exercised 5 days/week on a treadmill at a 5% incline for 6 weeks. By the end of the sixth week trained rats were required to run for 90 minutes at a treadmill speed of 30 m/min. Sedentary rats were placed on a stationary treadmill for an identical period of time as the trained rats throughout the investigation. Rats were killed *via* an intraperitoneal injection of pentobarbital sodium (180 mg/kg) 48 hours after the last training bout. Gastrocnemius muscles were rapidly dissected and frozen in liquid nitrogen. Mitochondrial biogenesis markers were examined using commercially available antibodies for PPAR-γ co-activator-1α (PGC-1α), mitochondrial transcription factor A (Tfam) and cytochrome c.

Exercise-training for 6 weeks significantly increased PGC-1α, Tfam and cytochrome c protein levels in gastrocnemius muscle of ExWater and ExAllo rats ($p < 0.05$). Interestingly, allopurinol did not alter the exercise-induced increases in these key mitochondrial biogenesis markers. No difference was observed in PGC-1α, Tfam and cytochrome c protein levels in SedAllo animals when compared to the SedWater controls.

The fact that inhibition of XO-induced production of ROS with allopurinol failed to attenuate the increase in mitochondrial biogenesis markers with exercise-training suggests that XO may not be an essential source of ROS responsible for the stimulation of skeletal muscle mitochondrial biogenesis with exercise-training. Given that vitamin C has been shown to attenuate the increase in mitochondrial biogenesis with exercise-training (Gomez-Cabrera *et al.*, 2008), further studies examining other ROS producing sites within skeletal muscle are required to determine which sources of ROS are involved with regulating skeletal muscle mitochondrial biogenesis during exercise-training.

Akimoto T, Pohnert SC, Li P, Zhang M, Gumbs C, Rosenberg PB, Williams RS, Yan Z. (2005) *Journal of Biological Chemistry* **280**: 19587-19593.

Gomez-Cabrera MC, Borrás C, Pallardó FV, Sastre J, Ji LL, Viña J. (2005) *Journal of Physiology* **567**: 113-120.

Gomez-Cabrera MC, Domenech E, Romagnoli M, Arduini A, Borras C, Pallardo FV, Sastre J, Viña J. (2008) *American Journal of Clinical Nutrition* **87**: 142-149.

No effect of statins or ezetimibe on fat metabolism during aerobic exercise in dyslipidaemic individuals

M.A. Matuszek[1] and R. Grant,[1,2] [1]School of Medical Sciences, University of New South Wales, NSW 2052, Australia and [2]Australasian Research Institute, Sydney Adventist Hospital, Wahroonga, NSW 2076, Australia.

Hypercholesterolaemic individuals are encouraged by health professionals to supplement lipid-lowering medication with regular exercise. However, studies in healthy normolipidaemic subjects have found that some lipid-lowering agents inhibit fat metabolism during prolonged aerobic exercise, which may lead to an increased reliance on carbohydrate stores and earlier fatigue (Eagles *et al.*, 1996; Head *et al.*, 1993). The current study investigated the effect of statins or ezetimibe on fat metabolism in dyslipidaemic individuals.

Method. All subjects received written approval from their doctor to participate in the study. A total of 21 subjects, consisting of 16 males and females taking a statin, and 5 females taking ezetimibe, were recruited. Subjects made a total of three visits to the laboratory. All subjects ceased lipid-lowering medication for 3 weeks prior to visit 1, at which they performed a submaximal exercise test on a treadmill to predict maximal oxygen uptake (VO_2max). Visit 2 continued in the absence of lipid-lowering medication whereas visit 3 occurred after subjects had resumed medication for a minimum of 3 weeks. The protocol for visits 2 and 3 were identical whereby subjects came to the laboratory after an overnight fast, a forearm vein was cannulated, and subjects were given a low fat 1 MJ carbohydrate meal. After 75 minutes, subjects walked on the treadmill at an intensity of 50% of their calculated VO_2max, corresponding to a 'brisk walk', for a period of 45 min. Blood (6 ml) was collected into ethylenediaminetetraacetic acid (EDTA) vacutainers immediately before the meal, immediately before exercise, and at time 15, 30, and 45 min of exercise. O_2 uptake and CO_2 expiration were measured using the ParvoMedic metabolic cart to determine the proportion of carbohydrate and fat metabolism. Data are reported as mean ± SEM and were analysed with SPSS using the paired sample t-test and repeated measures ANOVA.

Results. Subjects were moderately healthy with the following profile: age: 57 ± 2 yr, SBP: 124 ± 2 mmHg, DBP: 80 ± 2 mmHg, body mass index (kg/m^2): 28 ± 1, body fat: 30 ± 2% and VO_2max 32 ± 2 $ml.kg.min^{-1}$. Lipid-lowering medication resulted in a significant reduction in total cholesterol (5.7 ± 0.3 versus 4.1 ± 0.1 mmol/l (without and with statin)), (6 ± 0.2 versus 5.6 ± 0.2 mmol/l (without and with ezetimibe); and low density lipoprotein (LDL) (3.77 ± 0.2 versus 2.3 ± 0.1 mmol/l (without and with statin)); 4 ± 0.14 versus 3.7 ± 0.2 (without and with ezetimibe) ($p < 0.05$). Whilst there was a significant overall increase in the proportion of fat metabolism and decrease in the proportion of carbohydrate (CHO) metabolism and respiratory exchange ratio (RER) during the exercise session, % fat and CHO contribution and RER at time 15, 30, and 45 min did not differ in the presence compared to in the absence of either drug tested (see Table).

	time	+ statin	- statin	*p*	+ ezetimibe	- ezetimibe	*p*
% FAT	15 min	19 ± 2	19 ± 3	.950	22 ± 4	23 ± 5	.396
	30 min	31 ± 2	28 ± 3	.315	31 ± 5	29 ± 5	.425
	45 min	38 ± 2	37 ± 3	.850	33 ± 5	34 ± 5	.496
% CHO	15 min	82 ± 3	82 ± 3	.982	78 ± 4	77 ± 5	.418
	30 min	70 ± 2	74 ± 3	.182	70 ± 5	72 ± 5	.411
	45 min	62 ± 2	63 ± 3	.835	67 ± 5	66 ± 5	.489
RER	15 min	.93 ± .01	.93 ± .01	1.000	.92 ± .01	.92 ± .01	.587
	30 min	.90 ± .01	.91 ± .01	.180	.90 ± .01	.91 ± .01	.513
	45 min	.88 ± .01	.88 ± .01	.751	.87 ± .01	.89 ± .01	.606

Conclusion. These data indicate that neither statins nor ezetimibe decrease fat availability during exercise and do not appear to place increased demands on carbohydrate to reduce exercise tolerance.

Eagles CJ, Kendall MJ, Maxwell S. (1996) *British Journal of Clinical Pharmacology* **41:** 381-7.
Head A, Jakeman PM, Kendall MJ, Cramb R, Maxwell S. (1993) *Postgraduate Medical Journal* **69:** 197-203.

Hyperaemic responses to forearm exercise

T. Van der Touw and M. Cook, School of Science and Technology, University of New England, Armidale, NSW 2351, Australia. (Introduced by Dr Gudrun Dieberg)

The hyperaemic response to exercise commences within seconds of the onset of exercise, and reaches a steady-state level after several minutes of constant workload. Although a variety of mechanisms appear to be involved, the interplay between these mechanisms is complex and not fully understood.

Eight seated healthy adult male subjects (21.5 ± 0.9 years of age) performed single 1 s forearm contractions, as well as 2 minutes of rhythmic exercise consisting of forty 1 s forearm contractions with each contraction followed by a 2 s period of rest. Contractions were made by the dominant forearm at 20 and 40% of the maximum strength. Forearm blood velocity was measured with a transcutaneous ultrasound Doppler blood velocity probe placed over the distal brachial artery in the antecubital fossa. Doppler forearm blood velocity signals were averaged over entire cardiac cycles and expressed as changes above baseline levels. The blood velocity response from a single 1 s contraction was added to itself every 3 s over 2 minutes to obtain a theoretical forearm blood velocity response to rhythmic forearm contractions. This response was compared with the blood velocity response measured during 2 minutes of rhythmic forearm exercise at equivalent levels of contraction force.

The hyperaemic response to single 1 s forearm contractions lasted 6.8 ± 2.0 and 7.4 ± 2.5 s respectively for 20 and 40% maximum contractions. The peak change in forearm blood velocity measured during 2 minutes of rhythmic forearm contractions corresponded closely to theoretical values calculated from single 1 s forearm contractions (11.9 ± 5.3 and 11.9 ± 6.7 cm/s respectively at 20% maximum contractions, 17.7 ± 11.5 and 17.8 ± 7.1 cm/s respectively at 40% maximum contractions; both $p > 0.95$ with paired Students *t* tests). Forearm blood velocity during rhythmic exercise did not always reach a steady-state plateau during the 2 minutes of rhythmic exercise, and reached 80% of the steady-state theoretical plateau more slowly than predicted from the hyperaemic response to a single contraction (52.8 ± 29.1 and 9.8 ± 8.3 s at 20% maximum contractions, 29.2 ± 16.0 and 8.5 ± 3.2 s at 40% maximum contractions; both $p < 0.005$ with paired Students *t* tests).

The results suggest that a rapidly acting hyperaemic response is initially sufficiently potent to fully match increased metabolic demand during rhythmic forearm exercise. However, precise matching between blood flow and metabolic demand by the rapidly acting hyperaemic response theoretically occurs sooner than is actually observed during rhythmic exercise. We speculate that the rapid hyperaemic response diminishes in potency with repeated forearm contractions and that slower onset autoregulatory mechanisms are then brought into play to precisely match increased metabolic demand.

The response of isolated tunica dartos muscle to acute and prolonged cold stimulation and noradrenaline

I. Nanayakkara, S.K. Maloney and A.J. Bakker, Discipline of Physiology, School of Biomedical, Biomolecular and Chemical Sciences, University of Western Australia, WA 6009, Australia.

Human infertility is a problem affecting 10-15% of couples, with approximately equal contribution from both partners (DeKretser and Baker, 1999). Spermatogenesis is a temperature sensitive process that is regulated by the hypothalamo-pituitary gonadal axis of hormones. In most mammals testicular temperature is maintained 2-6°C below the core body temperature (Maloney & Mitchell, 1996). The tunica dartos muscle lining the scrotal skin plays an important role in the regulation of testicular temperature and therefore, male fertility. Contraction of the dartos reduces the surface area of the scrotum and the blood flow to the scrotal skin, preventing heat loss. Dartos relaxation causes excess heat to be removed (Shafik, 1973). Dartos contraction can be induced by sympathetic stimulation, and cold-induced contraction was previously thought to be mediated solely through a spinal reflex involving the sympathetic nerves and noradrenaline. However, cooling of the isolated dartos produces a contractile response indicating that other mechanisms also induce contraction in the dartos (Maloney *et al.*, 2005). Therefore, we have studied the contractile physiology of the isolated dartos muscle with regard to cold stimulation and noradrenaline.

Isolated dartos muscle strips (2-3 mm wide) were obtained from the glabrous part of the scrotum of Wistar rats and were connected using 3/0 surgical silk to a force transducer system in an organ bath. The tissue suspended organ chamber contained Krebs-Ringer solution (NaCl 121 mM, KCl 5.4 mM, $MgSO_4 \cdot 7H_2O$ 1.2 mM, $NaHCO_3$ 25 mM, HEPES 5 mM, glucose 11.5 mM, $CaCl_2 \cdot H_2O$ 2.5 mM) with a pH of 7.35. The bath was aerated with carbogen (5% CO_2 and 95% O_2) and its temperature was controlled via a recirculating water bath at 33°C.

The isolated dartos muscle contracted in response to electrical field stimulation, noradrenaline exposure and cooling to 15°C. The cooling response was greater with the overlying skin present, compared to the isolated muscle (115 ± 6.1% compared to 37 ± 7.3% of EFS response, $p = 3.03 \times 10^{-7}$, $n = 8$). The dose response curve to noradrenaline was sigmoidal with an EC_{50} of 10^{-5} M ($n = 6$). Prolonged cooling caused the tension to gradually decrease to baseline after approximately 3 hours, allowing the noradrenaline response at 15°C to be determined in the absence of cooling induced force. The contractile response to noradrenaline at 15°C was 153% of that measured at 33°C. The contractile reactivity to noradrenaline was decreased at higher temperatures, as previously shown by another method (Gibson et al., 2002). Repeated cooling (after rewarming) led to a marked reduction in the contractile response to further cooling (3^{rd} cooling peak tension 28.5 ± 11.7% of 1^{st} peak, $n = 6$). No such reduction in response was observed with repeated electrical field stimulation or noradrenaline.

This study shows that the cooling response in the tunica dartos is enhanced by the presence of the skin, and the cooling response may be in part due to greater sensitivity to basal noradrenaline release at lower temperatures.

DeKretser DM & Baker HW. (1999) *Journal of Clinical Endocrinology and Metabolism,* **84:** 3443-50.

Gibson A, Akinrinsola A, Patel T, Ray A, Tucker J & McFadzean I. *British Journal of Pharmacology,* **136:** 1194-200.

Maloney SK & Mitchell D. (1996) *Journal of Physiology,* **496:** 421-30.

Maloney SK, Shepherd KL & Bakker AJ. (2005) *Pflügers Archives - European Journal of Physiology,* **451:** 489-97.

Shafik A. (1973) *Investigative Urology,* **11:** 98-100.

Uterine spontaneous contractions in the estrous cycle and the effect of mitochondrial inhibitors

F.S. Gravina,[1] K.P. Kerr,[1] S. Sandow,[2] R.B. de Oliveira,[1] H.C. Parkington,[3] M.S. Imtiaz[1] and D.F. van Helden,[1]
[1]School of Biomedical Sciences, University of Newcastle, NSW 2308, Australia, [2]Department of Pharmacology, University of New South Wales, NSW 2052, Australia and [3]Department of Physiology, Monash University, VIC 3800, Australia.

Uterine smooth muscle plays an essential role in parturition. During labour the smooth muscle of the uterus contracts forcefully and rhythmically in order to deliver the newborn. In non-pregnant animals the uterus also contracts, possibly in response to the menstrual period or estrous cycle. Despite its importance, the mechanism of uterine contractions is not well understood. The role of Ca^{2+} stores in this process is still controversial. A recent study in the guinea pig gallbladder has shown that mitochondrial Ca^{2+} plays an essential role in tone and motility of this tissue (Balemba *et al.*, 2008). Preliminary studies on the uterus have shown that mitochondria may indeed play a role in uterine pacemaking (Gravina *et al.*, 2007).

The aim of the present study is: i) to determine the effect of the estrous cycle (estrus *vs* metestrus) on the spontaneous contractions; and ii) to compare the effects of mitochondrial inhibitors on the spontaneous contractions during different stages of the estrous cycle. Swiss mice (6-10 weeks) were euthanized by overexposure to the inhalation anaesthetic isoflurane (5-10% in air), a procedure approved by the Animal Care and Ethics Committee at the University of Newcastle. Vaginal smears were performed with NaCl 0.9% in order to determine the phase of the estrous cycle (Marcondes *et al.*, 2002). Uteri were dissected out and each one provided 4 pieces of uterine horn. These preparations were set up in 3 ml organ baths containing Krebs solution, bubbled with carbogen at 37°C, under 0.5 g wt tension to record the force developed by the longitudinally-arranged layer. Tissues were allowed to equilibrate for 20 minutes. The force of contractions was recorded isometrically from a Grass FT.03 tension transducer connected to a MacLab4e system. Log concentration-response curves were constructed using 3 different mitochondrial inhibitors: carbonyl cyanide 3-chlorophenylhydrazone (CCCP, a mitochondrial uncoupler), 7-chloro-5-(2-chlorophenyl)-1,5-dihydro-4,1-benzothiazepin-2(3H)-one (CGP37157, a mitochondrial Ca^{2+}/Na^{2+} exchange blocker) and oligomycin (an ATP synthase inhibitor). Spontaneous contractions during estrus were significantly different from metestrus (0.20 ± 0.02 g wt/mg, $n = 5$ *vs* 0.29 ± 0.02 g wt/mg, $n = 10$; $p < 0.05$). Spontaneous contractions were inhibited by CCCP (pIC50 = 5.78 ± 0.10, n = 5-10) and CGP37157 (pIC50 = 4.29 ± 0.10, n = 4-9). In contrast, oligomycin did not affect contractions (n = 4). CCCP did not have a significantly different effect in estrus (pIC50 = 6.17; 95% CI 5.61-6.73, n = 3) when compared with metestrus (pIC50 = 5.66; 95% CI 5.46-5.87, n = 3). However, the effect of CGP37157 was significantly different ($P<0.05$) between estrus (pIC50 = 3.65; 95% CI 3.21-4.09, n = 3) and metestrus (pIC50 = 4.38; 95% CI 4.14-4.62, n = 3).

In conclusion, this study reinforces our previous finding that mitochondria may play a role in uterine pacemaking, not only as an ATP producer (as oligomycin, an ATP synthase inhibitor, did not inhibit contractions, showing that the effects of the other drugs were not due to lack of ATP). Moreover, this study shows different sensitivities to at least one of these inhibitors depending on the estrous cycle.

Balemba OB, Bartoo AC, Nelson MT, Mawe GM. (2008) *American Journal of Physiology*, **294:** G467-76.
Gravina FS, Ryan K, Imtiaz M, Sandow S, Smith R, Parkington H, van Helden D. (2007) *Proceedings of the Australian Physiological Society*, **38:** 119P.
Marcondes FK, Bianchi FJ. Tanno AP. (2002) *Brazilian Journal of Biology*, **62:** 609-14.

The pacemaker and pattern generator underlying colonic migrating motor complexes does not require release of serotonin from the mucosa

D.J. Keating and N.J. Spencer, Department of Human Physiology, School of Medicine, Flinders University, SA 5001, Australia.

Introduction. Colonic migrating motor complexes (CMMCs) are cyclical contractions of the colonic smooth muscle layers which occur *in vivo* and *in vitro* and propagate over large distances along the large bowel, facilitating the propulsion of colonic contents. The location of the pacemaker that generates CMMC rhythmicity is unknown, but must lie within the colon itself, since CMMCs occur in an isolated whole colon. Data obtained from a number of laboratories strongly suggests that the activity of the CMMC pacemaker involves release of serotonin (5-HT) from the intestinal epithelium, since antagonists of the 5-HT_3 receptor slow the CMMC pacemaker and prolong intestinal transit, making these drugs effective in relieving the symptoms of diarrhea-predominant irritable bowel syndrome (D-IBS). What is not clear, is how or where the release of 5-HT from EC cells acts to control the CMMC pacemaker, or whether EC cells themselves even form part of the CMMC pacemaker mechanism. Since 5-HT is known to be released specifically from EC cells, we have correlated, in real time, the release of serotonin from EC cells, whilst recording CMMCs in isolated whole preparations of mouse colon.

Aim. To determine the role of endogenous serotonin release from EC cells in the generation and propagation of CMMCs.

Methods. Carbon fibre electrodes were used to record the dynamic release of 5-HT from a population of ECs in the mid colon, whilst at the same time, recordings were made of spontaneously occurring CMMCs propagating from the proximal to distal colon using isometric mechanical recording techniques. The whole colon was isolated from male C57BL/6 mice and a longitudinal incision made along the whole length. Two types of preparation were used: one type where the entire colon was intact and measurements of 5-HT release were made from EC cells, and a second type of preparation where the mucosa, submucosa and submucosal plexus were removed from the whole colon, and measurements of 5-HT release were made from the circular muscle.

Results. It was found that each CMMC contraction was commonly found to temporally correlate with a simultaneous release of 5-HT from the mid colon. To test whether the CMMC pacemaker required release of 5-HT from EC cells, we dissected off the mucosa, submucosa and submucosal plexus from the entire full length of colon. Removal of these structures abolished all cyclical rises in 5-HT release from the mucosa, but did not prevent the cyclical generation of CMMCs. Specifically, it was found that removal of the mucosa, submucosa and submucosal plexus caused a slight, but insignificant decrease in CMMC rhythmicity (control interval: 1.5 ± 0.27min; *c.f.* after mucosal removal: 2.0 ± 0.3min; n =4: $p = 0.26$), but no significant differences in CMMC amplitudes (control: 38.8 ± 11.1mN, *c.f.* without mucosa: 44.9 ± 7.6mN; n = 4: $p = 0.66$), or half durations (control: 14.7 ± 4.3 *c.f.* without mucosa: 18.3 ± 2.9s; n = 4; $p = 0.52$). All CMMC activity that persisted in preparations consisting of only myenteric ganglia and smooth muscle were abolished by hexamethonium 200μM; n = 3.

Conclusions. The pacemaker and pattern generator underlying the cyclical generation and propagation of CMMCs is located within the myenteric plexus, and does not require release of serotonin, nor any other endogenous substances from the colonic epithelium. Also, no evidence was found to suggest that intrinsic neural inputs from the submucosal plexus were required for CMMC generation or propagation.

Spatial relationships influence stimulus-secretion coupling in secretory epithelial cells

J. Low and P. Thorn, School of Biomedical Science, University of Queensland, QLD 4072, Australia.

Introduction. Stimulus secretion coupling in excitable cells primarily utilizes the influx of calcium through cell-surface calcium channels as the trigger for exocytosis. Work has characterized the spatial relationships between the calcium channels and the sites of exocytic release. Many secretory cells, however, do not use influx of calcium as the trigger for exocytosis and instead use calcium release from intracellular calcium stores. In these cells, and a good example is the pancreatic acinar cells, there is little information as to how the calcium release sites are spatially related to the sites of exocytosis. We know in these cells that exocytosis occurs exclusively along the lumen and that relatively high calcium concentrations are required to trigger exocytosis (Ito *et al.,* 1997). We also know that calcium release is focused at the lumen and this has led us to speculate that the calcium release apparatus may be closely apposed to the sites of exocytosis (Thorn *et al.,* 1993). Here we test this hypothesis.

Methods. Male CD-1 mice were killed according to the approved ethical procedures of The University of Queensland. The pancreas was excised and collagenase-digested to produce fragments of pancreatic tissue (see Thorn *et al.,* 2004 for details). The tissue fragments were bathed in fluorescent dye, sulforhodamine B (SRB) and imaged live with 2-photon microscopy. Cell exocytic responses were typically stimulated with cholesystokinin (CCK, 15 pM). Upon exocytosis the extracellular fluorescent dye enters and labels the granules. Cells were loaded with Fura-2 (AM) and the fluorescence recorded to determine the calcium response. Finally in some experiments we loaded the cells with NP-EGTA (caged calcium) and used a UV light source, with flash duration controlled electronically, to uncaged calcium within the cells.

Results. The first question we asked was, whether under conditions of uniform calcium elevation we could observe clustering in the sites of exocytic release. To characterize the exocytotic response we uncaged calcium from NP-EGTA. Varying the UV photolyisis flash duration (from 5 to 200 ms) released calcium in a graded manner (as recorded with Fura-2). At the shorter flash durations we observed limited to no exocytic activity. With the longest durations of 100 ms large calcium responses triggered massive exocytic responses (measured as events per lumen length per minute 1.61 events/nm/minute ± 0.35) with short latencies (9.459s ± 0.525). In these experiments the calcium signal rises uniformly across the cell. Spatial analysis of the exocytic response revealed a modal value for granule-to-granule distance apart of 3 μm with evidence to suggest that this distance is not due to any spatial localization of release sites but rather due to the limited lengths of the lumens in each cell. Further analysis showed that the latency of response was similar along the lumen length, reinforcing the idea of uniformity of exocytic release sites along the lumen.

We then asked the question as to whether, in response to CCK, where there is a clear structure to the calcium response, that this signal structure affected the spatial organization of exocytic responses. CCK-induced oscillations start at a specific locus within the apical region of the cell and then travel as a wave to all other regions of the cell. Past work suggests that these focal hot-spots of calcium release are due to regions of particularly active inositol trisphosphate receptors. Here we determined the focal hot-spot by a first derivative analysis of the calcium responses and recorded the exocytic responses, studying the latency to respond and the location of exocytosis. Measuring the distance between the focal hot-spot of release and the triggered exocytic responses revealed ~50% of granules are released within 4 μm of the calcium release site. Surprisingly, very few exocytic responses were seen < 1 μm from the calcium release hot-spot possibly suggesting steric exclusion of granular exocytosis.

Conclusions. We here describe for the first time the spatial relationship between the calcium signal and the exocytic response in cells primarily reliant on release of calcium from intracellular stores. Our data show that the exocytic release sites have no preferential clustering along the lumen. But we show that the structure of the agonist-evoked calcium response does influence the spatial extent of exocytic release.

Ito K, Miyashita Y & Kasai H. (1997) *EMBO Journal* **16:** 242-51.
Thorn P, Lawrie AM, Smith PM, Gallacher DV & Petersen OH. (1993) *Cell Calcium* **14:** 746-57.
Thorn P, Fogarty KE & Parker I. (2004) *Proceedings of the National Academy of Sciences USA* **101:** 6774-9

EGF and neurotensin mediated proliferation in HT-29 colon cancer cells; defining a role for the scaffold protein NHERF-1

W.A. Kruger,[1] Y. Jang,[1] G.R. Monteith[2] and P. Poronnik,[1] [1]School of Biomedical Science, University of Queensland, St Lucia, Qld 2072, Australia and [2]School of Pharmacy, University of Queensland, St Lucia, Qld 4072, Australia.

Cancer of the lower intestine or colorectal cancer is the most common cancer in Australia, with approximately 1 in 20 Australians being diagnosed with some form of colorectal cancer each year. Current treatment relies on surgery combined with chemotherapy or radiotherapy. A deeper understanding of the molecular basis for cellular dysfunction in colorectal cancer is essential to identify new targets for therapeutic intervention. Epidermal growth factor (EGF) and neurotensin (NT) are important pro-proliferative factors implicated in colorectal cancer cell proliferation. Our research focuses on the roles of the Na^+/H^+ exchanger regulatory factor 1 (NHERF-1) as a PSD-95/Dlg/Zo-1 (PDZ) scaffold in mediating cell signalling in epithelial cells. This protein plays a major role in scaffolding macromolecular complexes involved in signal transduction. Importantly, NHERF-1 has been shown to interact with the EGF receptor to cluster the receptor at the cell surface (Lazar *et al.*, 2004). This study was undertaken to investigate the role of NHERF-1 in EGF and neurotensin (NT) mediated proliferation of colorectal cancer cells. The HT-29 cell line was derived from a primary human adenocarcinoma of the rectosigmoid colon and is widely used as a model for colorectal cancer. The basic strategy was to use lentiviruses to deliver siRNA against NHERF-1 and to study the effects of silencing NHERF-1 on EGF and NT evoked Ca^{2+} signalling and cellular proliferation using biochemical and spectrophotometric techniques. Cells were infected with the virus for 2 days, serum starved for 2 days and treated with EGF or NT for 24 hours. To investigate the binding of NHERF-1 to a putative PDZ binding domain in the C-terminal tail of the type 1 neurotensin receptor (NTR-1) co-immunoprecipitation was used. Treatment of the cells with either EGF or NT increased the rate of proliferation by 30±2% (EGF) and 17±5% (NT) (n=4). When the cells were exposed to EGF and NT together no synergism was observed, suggesting that the two mitogens may act *via* similar signalling endpoints. Infection of HT-29 cells with the lentivirus expressing siRNA against NHERF-1 reduced endogenous levels of the protein by 80±5% (n=3) as determined by Western blot. MTT-assays demonstrated that silencing of NHERF-1 also reduced cell proliferation of cells grown in serum containing medium by 57±12% (n=5). In addition, in cells silenced for NHERF-1, neither EGF nor NT had any proliferative effect. NTR-1 is a G-protein coupled receptor that signals *via* increases in intracellular Ca^{2+}. In cells silenced for NHERF-1, the peak increase in Ca^{2+} was reduced by 70±5% (n=5) of the control, as determined using the Ca^{2+} sensitive dye Fluo-3. However, co-immunoprecipitation of a GFP-tagged fusion protein expressing the C-terminus of NTR-1 showed no detectable interaction to NHERF-1 in HT-29 cells.

These data demonstrate a key role for NHERF-1 as a positive regulator of HT-29 cells in response to serum, EGF and NT. The exact molecular basis for this effect remains to be determined but suggests a role for macromolecular signalling complexes scaffolded by PDZ proteins. Inhibition of NHERF-1 may be a target for the design of more specific anticancer therapies.

Lazar, C.S., Cresson, C.M., Lauffenburger, D.A. & Gill, G.N. (2004) *Molecular Biology of the Cell*, **15**, 5470-5480.

Megalin binds to NHERF1 and NHERF2 scaffold proteins

K.A. Jenkin,[1] C. Slattery,[2] P. Poronnik[2] and D.H. Hryciw,[1] [1]School of Biomedical and Health Sciences, St Albans, Victoria University, VIC 8001, Australia and [2] School of Biomedical Sciences, The University of Queensland, St Lucia, QLD 4069, Australia.

Albumin endocytosis in the renal proximal tubule is regulated by the scavenger receptor megalin, as well as a number of transmembrane and accessory proteins. Previously we have demonstrated an essential role for the scaffold proteins NHERF1 and NHERF2 in albumin uptake. NHERF1 and NHERF2 are PDZ domain containing proteins that interact with specific sequences that form a PDZ binding domain (S/TXΦ) in the C-terminus of transmembrane proteins. Interestingly, megalin contains a functional PDZ binding domain (SDV), however an interaction between meaglin and the scaffold proteins NHERF1 and NHERF2 has not been investigated.

In this study we will investigate if there is an interaction between megalin and NHERF1 and NHERF2, and then characterize the specific domains required for this interaction. Initially, immunoprecipitation experiments were performed using anti-megalin, anti-NHERF1 and anti-NHERF2 antibodies that were incubated with rat kidney lysate. The immunoprecipitates were analysed by Western blot analysis using the anti-NHERF1 and anti-NHERF2 and anti-megalin antibodies, respectively. These studies clearly indicated that megalin bound to NHERF1 and NHERF2 *in vivo*. To determine which domains in NHERF1 and NHERF2 were required for this interaction, GST fusion proteins were generated as described previously (Hryciw *et al.,* 2006; Lee *et al.,* 2007). These fusion proteins included the full length NHERF proteins as well as their 2 PDZ domains (PDZ1 and PDZ2) and C-terminal ezrin binding domain. Incubation with rat kidney lysate and analysis by Western blot analysis indicated that megalin bound to PDZ2 of NHERF1 and PDZ2 and the C-terminal ezrin binding domain of NHERF2. Megalin binds to NHE3, an exchanger that that is also essential for albumin endocytosis. Interestingly, NHE3 also binds to in NHERF1 and NHERF2 using the same PDZ binding domains.

We also investigated the distribution of megalin and NHERF1 and NHERF2 in the opossum kidney (OK) proximal tubule cell line. OK cells are a well characterized model of albumin endocytosis that contains a large number of essential endogenous proteins including megalin, NHE3, NHERF1 and NHERF2. Confocal analysis of OK cells demonstrated that the distribution of megalin was predominantly apical with some cytosolic localization. Importantly, NHERF1 had a strong apical localization which overlapped with megalin. Further, as previously described (Hryciw *et al.,* 2006) NHERF2 was predominantly cytosolic, and this protein co-localized with megalin in this region. Therefore, we have described for the first time an interaction between megalin and the scaffold proteins NHERF1 and NHERF2. As the NHERF proteins have been shown to be required for the formation of macromolecular complexes in other cell systems, further investigation should determine if they play a role for the complex formation required for the regulation of megalin medicated albumin endocytosis in proximal tubule cells.

Hryciw DH, Ekberg J, Ferguson C, Lee A, Wang D, Parton RG, Pollock CA, Yun CC, Poronnik P. (2006) *Journal of Biological Chemistry*, **281:** 16068-77.

Lee A, Rayfield A, Hryciw DH, Ma TA, Wang D, Pow D, Broer S, Yun C, Poronnik P. (2007) *Glia*, **55:** 119-29.

Identification of glutamate transporter glast splice variants in hypoxic neonatal pig brain

A. Lee,[1] S. O'Driscoll,[2] D. Pow[2] and P. Poronnik,[1] [1]School of Biomedical Science, University of Queensland, Brisbane, Qld 4072, Australia and [2]Centre for Clinical Research, University of Queensland, Royal Brisbane and Womens Hospital, Qld 4029, Australia.

Glutamate homeostasis is critical to normal brain function and deficiencies in regulation of extracellular glutamate are thought to be a major determinant of damage in hypoxic brains. Extracellular levels of glutamate are regulated mainly by plasma membrane glutamate transporters. In this study, RNA from hypoxic neonatal pig brains were analysed for isoforms of the glutamate transporter GLAST using reverse transcription PCR and cDNA cloning/sequencing methods. As reported previously in the human (Vallejo-Illarramendi *et al.*, 2005), a splice variant lacking exon 9 (GLASTex9skip) was also detected in hypoxic pig brain. Sequence alignment revealed that GLASTex9skip shared ~90% sequence similarity (at the nucleotide and amino acid level) with the human orthologue EAAT1ex9skip. We also isolated a novel splice variant which lacks both exons 5 and 6 (GLASTex5+6skip) resulting in the loss of 112 amino acids. RT-PCR analysis indicated that both these splice variants are expressed in the hypoxic brain, at levels ranging between 10% and 20% of the level of full length pig GLAST. Immunohistochemical analysis revealed that GLASTex9skip was expressed in the plasma membrane of neurons following mild hypoxic insult. Uptake studies using hypoxic brain slices demonstrated accumulation of a glutamate analogue (D-Glu) into neurons. This uptake of D-glu is unlikely to be due to EAAC1 (EAAT3), the only other candidate neuronal transporter of glutamate in the cortex since D-Glu is not a substrate for EAAC1. Furthermore, we observed no accumulation of D-Glu into neurons in brain slices from control animals that did not express GLASTex9skip. Our data support a model in which GLASTex9skip is a glutamate transporter in hypoxic neurons. We propose that the utilization of GLASTex9skip rather than a multi-step transport process (glutamate-glutamine cycle) with multiple energy demands may be an adaptation of the brain to reduce energy burden while maintaining glutamate homeostasis, at least under conditions of low energy availability. Further *in vitro* transport studies are underway using cloned GLASTex9skip and GLASTex5+6skip to characterise the glutamate transporting capacity of these GLAST isoforms.

Vallejo-Illarramendi A, Domercq M, Matute C. (2005) *Journal of Neurochemistry* **95**: 341-348.

Protons released as a by-product of exocytosis affect the intracellular calcium response

N. Behrendorff and P. Thorn, School of Biomedical Sciences, University of Queensland, St Lucia, QLD 4072, Australia.

Introduction. Most, if not all, secretory granules maintain an acidic pH. In many types of granules this is used to drive secondary-active uptake of contents into the granule (*eg.* neurotransmitter uptake). In peptidergic granules the acid lumen is thought to act as a charge screen between the proteins enabling a tighter packing of granule contents. With granule fusion during exocytosis, protons are lost through the open fusion pore prior to the loss of other, heavier granule content. The loss of the acid gradient is one of the first events of exocytosis. Given the high mobility of the protons, release from a small granule into a large extracellular volume would be expected not to change the extracellular pH significantly. Where the extracellular environment is restricted, this might not be the case. Within hollow organs, it is conceivable that exocytotic release of protons from granules might contribute to the intra-organ pH environment. In organs with a restricted extracellular volume, regulated pH changes have been shown to occur as a result of the transport of acid into the extracellular environment (Chu & Montrose, 1995). Here we report our results on whether exocytosis can lead to pH changes in the lumen of the exocrine pancreas.

Methods. Male CD-1 mice were killed according to the approved ethical procedures of The University of Queensland. The pancreas was excised and collagenase-digested to produce fragments of pancreatic tissue (see Thorn & Parker, 2005). The tissue fragments were bathed in extracellular fluorescent dyes and imaged live with 2-photon microscopy. Cell exocytic responses were stimulated with cholecystokinin (20 or 100 pM). Upon exocytosis the extracellular fluorescent dye enters and therefore labels the granules. We used two different extracellular dyes; sulforhodamine B (SRB, an inert dye), 8-Hydroxypyrene-1,3,6-trisulfonic acid (HPTS, a pH sensitive dye, see Schwiening & Willoughby, 2002) and 8-Methoxypyrene-1,3,6-trisulfonic acid (MPTS used as an inert control for HPTS). We also used an intracellular calcium sensor, Fluo-4 AM. We calibrated the pH sensitivity of HPTS in the 2-photon microscope with 950 nm excitation light. Our estimated Kd, derived from the calibration was 6.79.

Results. Initial experiments were performed in the presence of extracellular 7 mM HEPES. Here we observed single exocytic events in response to 20 pM CCK. These events were seen as a sudden increase in SRB and HPTS fluorescence in the granule. In regions of interest in the lumens, immediately adjacent to the exocytic events, we observed little change in the SRB signal (in some cases a small increase due to dye binding to released proteinaceous content – see Thorn & Parker, 2005). In contrast, we consistently observed small, transient decreases in HPTS fluorescence indicative of possible acidification. Applying our HPTS calibration to this data gave us an estimated mean decrease from 7.4 to 7.24 ± 0.03 (n = 68). To assess the unbuffered pH changes we removed HEPES from the extracellular solution. Again the luminal SRB changes were small or showed a slight increase. Now HPTS recorded greater pH changes (from 7.4 to a mean of 7.02 ± 0.03 n = 52). These luminal changes preceded the influx of SRB into the granule suggesting release of protons from the granule through an initial fusion pore too small to allow SRB entry. Control experiments with MPTS showed no changes. Experiments stimulating the cells with high CCK (100 pM) showed dramatic luminal acidifications. To determine if these extracellular pH changes affected cell responses we measured cytosolic calcium responses to CCK (with Fluo-4 AM) +/- extracellular HEPES. The responses were very different. For example the frequency of calcium oscillations in HEPES was 0.42 ± 0.03 Hz (n = 43) compared to 0.65 ± 0.06 Hz (n = 38) in the absence of HEPES (p < 0.001), supporting the idea that extracellular pH changes do have functional consequences for the cell.

Conclusions. What we show here is that proton release from secretory granules significantly acidifies the primary secretory output with pH drops of up to 0.4 pH units. This several fold increase in protons is an unprecedented change for an extracellular ion and we show this pH change is capable of modulating intracellular calcium levels. We conclude that the acid content of secretory granules has the potential for significant effects when released.

Chu S & Montrose M. (1995) *Proceedings of the National Academy of Sciences USA*, **92:** 3303-7.
Schwiening C & Willoughby D. (2002) *Journal of Physiology* **538:** 371-82.
Thorn P & Parker I. (2005) *Journal of Physiology* **563:** 433-42.

Epithelial Sodium channels are regulated by the tyrosine kinase, c-Abl

S.H. Song, I.H. Lee, A. Dinudom and D.I. Cook, Discipline of Physiology, School of Medical Science, Faculty of Medicine, University of Sydney, Sydney, New South Wales 2006, Australia..

Epithelial Na^+ channels (ENaC) mediate Na^+ absorption in kidney, lung and colon epithelia. The function of ENaC is important in the maintenance of Na^+ and fluid homeostasis, and the regulation of plasma volume and blood pressure. Activity of ENaC is controlled by hormones, such as aldosterone and insulin, and paracrine signalling molecules, such as tumor necrosis factor (TNF) and transforming growth factor-β (TGF-β). Many of these regulators of ENaC activity exert their effects via protein kinases. Abelson kinase, c-Abl, is a 150-KDa non-receptor tyrosine kinase that is stimulated by two regulators of ENaC, TNF and TGF-β. c-Abl contains multiple interactive domains, including Src homology (SH) 3 domain and SH2 domain, a tyrosine kinase catalytic domain, proline-rich motifs, DNA-binding domains and actin-binding domains, which allow transduction of a variety of cellular signals. Although c-Abl is wildly expressed in epithelial cells, the role of this kinase in regulating ENaC is currently unknown.

Using RT-PCR and Western blot analysis, we confirmed endogenous expression of c-Abl kinase in mouse kidney collecting duct (M1) cells, human lung epithelial (H441) cells, and in Fisher rat thyroid (FRT) cells. We found that expression of a constitutively active mutant of c-Abl strongly inhibited the activity of ENaC in both M1 cells, which endogenously express ENaC and FRT cells which express exogenous ENaC. Interestingly, c-Abl cannot downregulate activity of a mutated ENaC in which the c-terminal of the β-subunit of the channel has been truncated, or a mutated ENaC in which a consensus phospholylation site for c-Abl on βENaC, βY618, is mutated to alanine. The amino acid Y618 on βENaC is part of the PY motif that interacts with the ubiqitin protein ligase, Nedd4-2, a known regulator of ENaC which mediates ubiquitin-dependent downregulation of the channel. c-Abl, however, downregulated activity of ENaC in cells in which Nedd4-2 expression was knocked-down by expression of siRNA directed against Nedd4-2.

We conclude that c-Abl kinase mediates its inhibitory effect on the activity of ENaC activity via the PY motif of the β-subunit of ENaC in a Nedd4-2 independent manner.

Regulation of the rat glutamine transporter SNAT3

S. Balkrishna, A. Bröer, A. Kingsland and S. Bröer, School of Biochemistry and Molecular Biology, The Australian National University, Canberra, ACT 0200, Australia.

Glutamine is the most abundant amino acid in the blood plasma and cerebrospinal fluid. It plays an essential role in neurotransmitter recycling in the brain, ammonia detoxification in the liver, and the compensation of metabolic acidosis in the kidney (Mackenzie & Erickson, 2004). In these organs, the uptake and release of glutamine is primarily carried out by the Sodium Neutral Amino Acid Transporter 3 (SNAT3) (Chaudhry *et al*., 1999). Due to this pivotal role played by SNAT3, an understanding of its regulation has high physiological relevance. Glutamine transport by SNAT3 is known to be accompanied by the co-transport of a sodium ion and the antiport of a proton in *Xenopus laevis* oocytes (Bröer *et al*., 2002). In this study, the regulation of the rat SNAT3 transporter by Protein Kinase C (PKC) was investigated. Activation of PKC by the treatment of oocytes expressing rSNAT3 with the phorbol ester PMA resulted in the rapid down-regulation of rSNAT3 activity. Mutational analysis of putative PKC phosphorylation sites showed that this down-regulation was not due to the phosphorylation of rSNAT3 at PKC specific sites. In order to investigate the cause of the down-regulation of rSNAT3 activity, confocal microscopy on oocytes expressing eGFP-rSNAT3 was performed. These studies revealed that the PMA-mediated regulation of the transporter was due to the retrieval of the fusion protein from the oocyte plasma membrane. Preliminary data indicate that this retrieval occurs through a dynamin-independent pathway.

Broer A, Albers A, Setiawan I, Edwards RH, Chaudhry FA, Lang F, Wagner CA, & Bröer S. (2002) *Journal of Physiology*, **539:** 3-14.

Chaudhry FA, Reimer RJ, Krizaj D, Barber D, Storm-Mathisen J, Copenhagen DR & Edwards RH. (1999) *Cell*, **99:** 769-80.

Mackenzie B & Erickson JD. (2004) *Pflügers Archive European Journal of Physiology*, **447:** 784-95.

Distribution of the amino acid transporters B^0AT1, B^0AT2 and ASCT2 in kidney and intestine

N. Tietze,[1] J.M. Vanslambrouck,[2] J.E.J. Rasko[2] and S. Bröer,[1] [1]School of Biochemistry and Molecular Biology, The Australian National University, Canberra, ACT 0200, Australia and [2]Gene and Stem Cell Therapy Program, Centenary Institute of Cancer Medicine and Cell Biology, University of Sydney, NSW 2050, Australia.

Dietary protein is almost completely absorbed in the intestine with the aid of proteases, peptidases, amino acid and peptide transporters. Plasma amino acids are filtered in the kidney and subsequently reabsorbed in the proximal tubule of the kidney. Neutral amino acids are transported in these tissues mainly by an amino acid transports activity referred to as System B^0. Three different amino acid transporters have been suggested to be member of this transport activity, namely B^0AT1 (SLC6A19), B^0AT2 (SLC6A15) and ASCT2 (SLC1A5). B^0AT1 is a Na^+ dependent, Cl^- independent and pH sensitive transporter, mediating transport of all neutral amino acids with low affinity (Bröer *et al.*, 2004). Further studies revealed a cotransport stoichiometry of 1 Na^+ together with a substrate (Bohmer *et al.*, 2005). ASCT2 mediates transport of neutral amino acids with the exception of aromatic amino acids with high affinity. It is a Na^+ dependent, electroneutral antiporter (Kekuda *et al.*, 1996; Bröer *et al.*, 2000; Avissar *et al.*, 2001). B^0AT2 has been characterized as a Na^+ dependent neutral amino acid transporter preferring branched-chain amino acids and proline with high affinity via the same mechanism as B^0AT1 (Takanaga *et al.*, 2005; Bröer *et al.*, 2006). In early studies B^0AT 2 was only detected in the brain but was subsequently also reported in kidney (Bröer *et al.*, 2006). However, its specific localisation in the kidney still needs to be elucidated and could give conclusion about function and possible compensation for other transporter malfunction. While low affinity transporters for neutral amino acids are found in the early (S1-S2) segments of the kidney, high affinity transporters have been reported in the later (S3) segments. Localisation of the B^0AT2 transporter would thus contribute to the understanding of amino acid reabsorption in the kidney.

In this study, the distribution of the neutral amino acid transporters B^0AT1, B^0AT2 and ASCT2 were investigated in kidney and intestine. Specific antibodies against these amino acid transporters were analysed in Western Blots, showing specific bands for brush border membrane vesicles and oocyte membrane preparations expressing the transporters. Immunofluorescence studies localised B^0AT1 in the apical membrane of the intestine and the proximal tubule of the kidney. B^0AT2 was found to be localised in a different part of the proximal tubule than B^0AT1. ASCT2 appears to be located in the distal tubule or in parts of the proximal tubule of the kidney.

Avissar NE, Ryan CK, Ganapathy V, Sax HC. (2001). *American Jounal of Physiology*, **281:** C963-71.

Bohmer C, Brer A, Munzinger M, Kowalczuk S, Rasko JE, Lang F, Bröer S. (2005). *Biochemical Journal*, **389:** 745-51.

Bröer A, Klingel K, Kowalczuk S, Rasko JE, Cavanaugh J, Bröer S. (2004). *Journal Biological Chemistry*, **279:** 24467-76.

Bröer A, Tietze N, Kowalczuk S, Chubb S, Munzinger M, Bak LK, Bröer S. (2006). *Biochemical Journal*, **393:** 421-30.

Bröer A, Wagner C, Lang F, Bröer S. (2000) *Biochemical Journal*, **346:** 705-10.

Kekuda R, Prasad PD, Fei YJ, Torres-Zamorano V, Sinha S, Yang-Feng TL, Leibach FH, Ganapathy V. (1996). *Journal Biological Chemistry*, **271:** 18657-61.

Takanaga H, Mackenzie B, Peng JB, Hediger MA. (2005) *Biochemical and Biophysical Research Communications*, **337:** 892-900.

Human sarcopenia reveals an increase in SOCS-3 and myostatin and a reduced efficiency of Akt phosphorylation

B. Léger,[1] W. Derave,[2] K. De Bock,[3] P. Hespel[2] and A.P. Russell,[4] [1]Institut de recherche en réadaptation-réinsertion, Avenue de Grandchampsec 90, Sion 1951, Switzerland, [2]Research Centre for Exercise and Health, Faculty of Kinesiology and Rehabilitation Sciences, K.U.Leuven, B-3001, Belgium, [3]Department of Movement and Sport Sciences, Ghent University, Ghent, Belgium and [4]The Centre for Physical Activity and Nutrition Research (C-PAN), School of Exercise and Nutrition Sciences, Deakin University, VIC 3125, Australia.

Introduction. Sarcopenia is the general term for a reduction in muscle quality and function due to aging. This can be seen by an increase in muscle atrophy, often in type II fibres, which is related to the reduction of maximal voluntary strength. Sarcopenia has an important socio-economic consequence as falls are a major source of morbidity and mortality in the increasing population of the elderly. Findings in the literature have prompted us to hypothesise that human sarcopenia may be linked to increased levels of in TNFα and SOCS3; the latter causing perturbations in GH signalling and increasing myostatin. Consequently, this would result in a reduced phosphorylation and activation of Akt signalling and therefore inhibit and activate respectively, muscle hypertrophy and atrophy signalling cascades. The aims of the present study were to determine if age-related sarcopenia in humans was linked with perturbations in TNFα, SOCS3, GH, STAT5 and IGF levels as well decreases in the Akt/GSK/mTOR and increases in the Akt/FKHR/atrogene signalling pathways.

Methods. This study investigated the regulation of several genes and proteins involved in the activation of key signaling pathways promoting muscle hypertrophy including GH/STAT5, IGF-1/Akt/GSK-3β/4E-BP1 and muscle atrophy including TNFα/SOCS3 and Akt/FKHR/atrogene, in muscle biopsies from 13 young (20 ± 0.2 years) and 16 older (age, 70 ± 0.3 years) males.

Results. In the older, when compared with the young subjects, muscle fibre cross sectional area was reduced by 40-45% in the type II muscle fibres. TNFα and SOCS-3 were increased by 2.8 and 1.5 fold respectively. Growth hormone receptor protein (GHR) and IGF-1 mRNA were decreased by 45%. Total Akt, but not phosphorylated Akt, was increased by 2.5 fold. This corresponded to a 30% reduction in the efficiency of Akt phosphorylation in the older subjects. Phosphorylated and total GSK-3β was increased by 1.5 and 1.8-fold respectively, while 4E-BP1 levels were not changed. Nuclear FKHR and FKHRL1 were decreased by 73 and 50%, with no changes in their atrophy target genes, atrogin-1 and MuRF1. Myostatin mRNA and protein levels were significantly elevated by 2 and 1.4 fold.

Conclusion. This is the first study to compare the regulation of several key signalling pathways, known to control skeletal muscle hypertrophy, including GH/STAT5, IGF-1/Akt/GSK/4E-BP1, and skeletal muscle atrophy, including TNFα/SOCS3 and Akt/FKHR/atrogene, in muscle biopsies from young and old men. It appears that human sarcopenia is associated with an increase in TNFα and SOCS-3 which may result in a reduction of GHR levels or sensitivity. The significant increase in total Akt protein content, but not in Akt phosphorylation, in muscle from the older subjects, suggests an inefficiency in Akt activation and by analogy reduced protein synthesis. The observed increase in myostatin mRNA and protein levels in the older subjects, combined with recent observations in cardiac and rodents cells (refs), suggest that myostatin is a prime candidate inhibiting Akt phosphorylation in the elderly. Establishing if this is the case should be a priority for future investigations aimed at reducing human sarcopenia.

Deschenes MR. (2004) *Sports Medicine*, **34:** 809-24.

Greiwe JS, Cheng B, Rubin DC, Yarasheski KE & Semenkovich CF. (2001) *Faseb Journal*, **15:** 475-82.

Liu W, Thomas SG, Asa SL, Gonzalez-Cadavid N, Bhasin S & Ezzat S. (2003) *Journal of Clinical Endocrinology Metabolism*, **88:** 5490-6.

Mahoney J, Sager M, Dunham NC & Johnson J. (1994) *Journal of American Geriatric Society*, **42:** 269-74.

Morissette MR, Cook SA, Foo S, McKoy G, Ashida N, Novikov M, Scherrer-Crosbie M, Li L, Matsui T, Brooks G & Rosenzweig A. (2006) *Circulation Research*, **99:** 15-24.

Contribution of Nitric Oxide to vagal nerve function in the dystrophin deficient heart

M. Watson, E. Lee and A. Hoey, Centre for Systems Biology, University of Southern Queensland, Toowoomba, QLD 4350, Australia.

Duchenne muscular dystrophy (DMD) causes alterations in structure and function leading to cardiac failure. The lack of neuronal nitric oxide (NO) in the myocardium has been implicated in some of the cardiac pathologies seen in DMD. Neuronal NO has also been implicated in the control of the vagus nerve supplying the myocardium. The aim of the current study was to investigate the *in vivo* function of the vagus nerve in reducing heart rate (HR) in *mdx* mice and if alterations in NO signaling can modulate vagal nerve function.

Mice were anaesthetized with ketamine (100mg/kg) and xylazine (5 mg/kg) and the right vagus nerve exposed and stimulated at 1, 2 and 5 V at 1, 2, 5, 10 and 20 Hz. Electrocardiogram (ECG), heart rate (HR), heart rate variability (HRV) and cGMP levels were examined using an ELISA assay.

Young (12 week) and old (12 month) *mdx* mice had significantly elevated basal HR, while old *mdx* mice had prolonged QTc interval, a significant reduction in SDNN (standard deviation of N-N intervals) and in the high frequency (HF) domain. Young and old *mdx* mice had a significant reduction in the HR response to vagal nerve stimulation (VNS). 5% L-Arginine (w/v drinking water) and 25% isosorbide dinitrate (ISDN, 25% w/v water food) for four days had no effect on basal ECG parameters but significantly improved HRV. Furthermore, the response to HR reduction following VNS was significantly improved throughout the stimulation regimes. This was associated with an increase in the level of cGMP levels in the treatment groups. These results suggest that *mdx* mice have tachycardia and an impaired autonomic function while administration of compounds that elevate NO improve vagal nerve function.

Phase resolved retardation measurements of isolated cardiomyocytes

N.M. Dragomir,[1] C.L. Curl,[2] A. Roberts[1] and L.M.D. Delbridge ,[2] [1]School of Physics, University of Melbourne, Vic 3010, Australia and [2]Department of Physiology, University of Melbourne, Vic 3010, Australia.

Quantification of the physical and optical properties of the fine structural information of transparent or translucent unstained anisotropic viable cellular specimens is challenging. The isolated cardiomyocyte is a particularly good example of such an anisotropic specimen, where the optical properties are different according to direction of measurement. Phase and retardation measurement are two optical quantities that provide information regarding structural properties. The phase contains information about cell thickness and refractive index. The retardation contains information about the cell thickness and the birefringence, which is a result of more than one index of refraction. Birefringence is highly dependent on biological, physiological and environmental conditions and is responsible of the orderly local arrangement of the thick (myosin) and thin (actin) filaments in the myofibrils of the cardiomyocyte. Phase measurement, performed using Quantitative Phase Microscopy (QPM), was used in conjunction with retardation measurement, performed using Brace-Köhler (BK) compensator.

Freshly isolated ventricular cardiac myocytes were obtained from male Sprague-Dawley rats by a standard enzymatic digestion procedure. Myocytes were suspended in two different buffer solutions (pH 7.4): one containing 2,3-butanedione monoxime (BDM), and the other containing 1mM Ca^{2+}.

Cells of appropriate dimensions (~28 × 125 μm) and shape exhibiting clear cross striations were analysed within 1.5hrs post isolation. Phase images were computed from a set of through-focus bright field images obtained using an *Olympus BX51* polarised microscope (40×/0.70 P, ∞/0.17 Uplan FL objective). Phase calculations were performed using QPm software (QPm^{Tm} V2.1 IATIA, Ltd.). Retardation was determined using BK method by observing the cells oriented at 45 ± 1° under linearly crossed polarisers mode while quantifying the azimuth orientation of a specialized compensator wave-plate of known retardation.

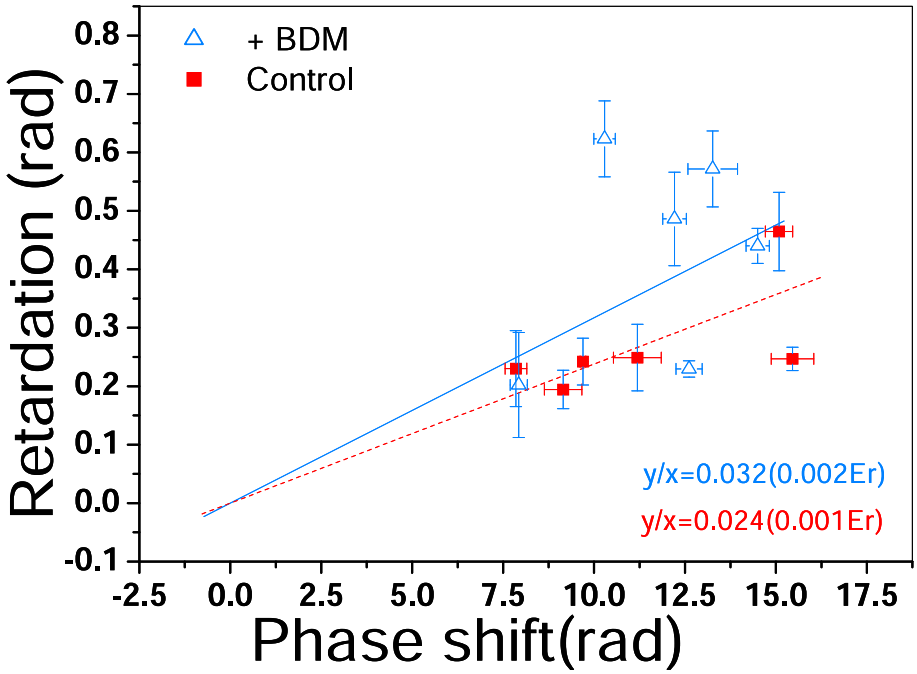

A positive correlation was observed between the retardation and the phase of the cardiomyocytes as illustrated by the linear regression curves fitted for cells placed in BDM (solid line) and control (dash line) buffers (see Figure). Moreover, cells placed in BDM 'relaxing' solution exhibited higher retardation magnitude than cells in control, 1mM Ca^{2+}, solution, despite the lower phase values. Thus myocyte birefringence as evaluated by retardation is affected by a pharmacologic treatment which alters the interaction between cytoskeletal elements. By contrast, phase is less affected by this treatment. For cells in either buffer, the retardation magnitude increased proportionally with increasing the thickness (i.e. phase) as expected.

An optimized RNA extraction protocol for stored human myocardial tissue biopsies

W.T.K. Ip,[1] C.E. Huggins,[2] S. Pepe[3] and L.M.D. Delbridge,[1] [1]Cardiac Phenomics Laboratory, Department of Physiology, University of Melbourne, Parkville, VIC 3010, Australia, [2]School of Exercise & Nutrition Sciences, Deakin University, Burwood, VIC 3125, Australia and [3]Murdoch Children's Research Institute, Department of Cardiology, Royal Children's Hospital, Parkville, VIC 3010, Australia.

Human cardiac tissue samples are valuable and availability is limited. Tissue acquisition for batch assay can be protracted and long periods (months to years) can elapse between sample collection and experimental analyses. This is a particular concern for gene expression studies where extended tissue storage may result in RNA degradation, making the tissue unsuitable for PCR analysis. RNA degradation may also occur due to sample exposure to RNases during the RNA extraction process. In order to ensure that real-time PCR results generated from these valuable human samples are reflective of biological difference and not a result of sub-optimal sample preparation method, we have investigated the effects of extended tissue storage and RNA preparation methods on RNA quality and downstream real-time PCR gene amplification. To examine the effects of extended tissue storage on sample quality, right atrial appendages (free from right heart disease) collected from patients undergoing coronary artery bypass surgery and stored at -80ºC for 5 years ('archived') and for up to 1 year ('recent') were compared. RNA extraction was performed using the Qiagen RNeasy® Fibrous Tissue Midi kit. RNA quality was assessed based on the 28S:18S ratio, and the RNA Integrity Number (RIN) - a score ranging from 1 (most degraded) to 10 (most intact). The effects of RNA quality on downstream PCR amplification (real-time PCR) of rRNA and mRNA genes were investigated. RNA recovery was not different between the archived and recent samples (6.70 ± 1.87 *vs* 6.93 ± 1.99 mg total RNA, $p > 0.05$). No differences were found in the RNA integrity measurements including the 28S:18S ratio (2.43 ± 0.17 *vs* 2.50 ± 0.17, $p > 0.05$), and RIN (9.33 ± 0.42 *vs* 9.22 ± 0.25, $p > 0.05$), suggesting that the archived samples were similarly intact compared to the recent samples. This was supported by real-time PCR data where the archived and recent samples were found to exhibit similar amplification of 18S and GAPDH (18S amplification efficiency: 1.48 ± 0.10 *vs* 1.48 ± 0.06, $p > 0.05$; GAPDH amplification efficiency: 1.86 ± 0.01 *vs* 1.86 ± 0.00, $p > 0.05$).

The second aim of this study was to investigate the effects of RNA extraction method on RNA integrity and real-time PCR gene amplification. Frozen human atrial appendages were pulverized using mortar and pestle and divided into two 100 mg portions to allow parallel comparison of the RNA preparation obtained using: 1) a 'multi-step' protocol - where RNA was extracted using phenol/chloroform (TRIzol® Reagent, Invitrogen), followed by DNase treatment (Deoxyribonuclease I - amplification grade, Invitrogen) and purification (MinElute® Cleanup kit, Qiagen); or 2) a 'single-step' protocol – where RNA was extracted using silica membrane based RNA extraction kits (RNeasy® Fibrous Tissue Midi kit, Qiagen), involving on-column DNase treatment and sample purification as part of the protocol. Comparison of RNA preparations extracted using the two methods revealed that the single-step preparations exhibited higher RNA integrity (28S:18S ratio = 1.38 ± 0.12 *vs* 2.50 ± 0.17, $p < 0.05$; RIN = 7.06 ± 0.70 *vs* 9.22 ± 0.25, $p < 0.05$). Consistent with the differences in RNA quality, multi-step samples were found to exhibit compromised GAPDH (mRNA) amplification, while 18S was unchanged. In summary, we have demonstrated that human atrial tissue samples that have been stored at -80ºC for up to 5 years are suitable for PCR gene expression study. In addition, we have established that the single-step RNA extraction method (using silica membrane based RNA extraction kits) is more suitable for human cardiac tissues. These findings suggest that the choice of RNA extraction method is critical and can markedly affect RNA quality and compromise downstream real-time PCR outcomes.

Concentration dependent modulation of the cardiac ryanodine receptor by Homer1

P. Pouliquin, S.M. Pace and A.F. Dulhunty, Division of Molecular Bioscience, JCSMR, ANU, Canberra, ACT 2601, Australia.

Calcium signalling controls a wide variety of physiological processes and depends on the activity of protein signalling complexes clustered in specialised cellular sites. Ryanodine receptor (RyR) calcium release channels form the hub of the calcium signalling complex that is vital in muscle contraction. Homer proteins allow both clustering and functional modulation of a plethora of proteins from different calcium signalling complexes; interactions between the ryanodine receptors and Homer emerge as a new aspect of regulation of the crucial calcium signal in muscle. Homer1 modulates the sekeletal ryanodine receptor (RyR1) activity in a concentration dependent manner (Feng *et al.*, 2008), activating the receptor at ≤ 200nM, but strongly inhibiting its activity at concentrations > 200nM. Only one publication has specifically examined the effect of Homer1 on the cardiac ryanodine receptor (RyR2, the main ryanodine receptor isoform in the heart and in the brain), concluding that Homer1 inhibits channel activity, regardless of its concentration (Westhoff *et al.*, 2003). Here we re-examine the modulation of the RyR2 activity by Homer1 and test the hypothesis that modulation of RyR1 and RyR2 by Homer1 are fundamentally different.

Skeletal and cardiac muscle sarcoplasmic reticulum vesicles were isolated from New Zealand rabbits or sheep heart, respectively. Human recombinant Homer1b (a long isoform able to multinerise) and short Homer (an isoform unable to multimerise) were purified by affinity chromatography. We determined the activity of the RyRs by two different means: specific [^{3}H]-ryanodine binding, which is proportional to the activity of a population of RyRs; and single channel techniques. With the later we measure the ionic current flowing through a single channel molecule incorporated in an artificial lipid bilayer where the solutions bathing each sides of the channel can be manipulated and the intrinsic gating properties of individual channels measured.

Homer1b increased RyR1 and RyR2 activity at all cytosolic [Ca^{2+}] without altering the [Ca^{2+}]-dependence. At resting and activating cytosolic [Ca^{2+}], Homer1b activated RyR2 in a dose dependent manner. In the presence of 1μM cytosolic Ca^{2+}, 50nM Homer1b increased RyR2 open probability (from 0.009 ± 0.003 to 0.137 ± 0.053) and mean open time (from 0.57 ± 0.09ms to 1.85 ± 0.46ms) without a significant change in mean closed time. Maximum activity was reached with ~50-100nM Homer1b, and activity fell dramatically with Homer1b > 200nM. When RyR2 was maximally activated by 100μM cytosolic Ca^{2+}, RyR2 activation by Homer1b was reduced, while inhibition by ≥ 200nM Homer1b was sustained. Short Homer1 similarly modulated RyR2 activity in a biphasic manner, though with lower affinity than Homer1b.

We conclude that Homer1 modulates skeletal RyR1 and cardiac RyR2 in an intrinsically similar manner. RyR2 modulation by Homer1b is likely to be physiologically relevant in the heart and in neurons, where high levels of the two proteins are expressed.

Feng W, Tu J, Pouliquin P, Cabrales E, Shen X, Dulhunty A, Worley PF, Allen PD, Pessah IN. (2008) *Cell Calcium*, **43:** 307-14.

Westhoff JH, Hwang SY, Duncan RS, Ozawa F, Volpe P, Inokuchi K, Koulen P. (2003) *Cell Calcium*, **34:** 261-9.

F157A and Y160A substitutions in the helix 6 Region of GSTM2-2 C terminus reduces the inhibitory action of helix 6 on RyR2 channels

R. Hewawasam, D. Liu, M.G. Casarotto, P.G. Board and A.F. Dulhunty, Division of Molecular Bioscience, The John Curtin School of Medical Research, Australian National University, ACT 2601, Australia.

The ryanodine receptor (RyR) Ca^{2+} release channel, located in the membrane of the internal sarcoplasmic reticulum Ca^{2+} store, is central to Ca^{2+} signalling and contraction in skeletal and cardiac muscle (Abdellatif *et al.*, 2007). Some glutathione transferases (GSTs) and structurally related proteins are potent modulators of ryanodine receptor (RyR) Ca^{2+} release channels. Recently it was discovered that muscle specific GSTM2-2 inhibits cardiac muscle ryanodine receptors (RyR2), but not skeletal muscle ryanodine receptors (RyR1) (Dulhunty *et al.*, 2001). The selective inhibition of RyR2 by GSTM2-2 has significant clinical potential in the treatment of chronic heart failure. Data obtained thus far suggests that the main inhibitory effect of GSTM2-2 on RyR2 is associated with α-helix 6. Since the flexibility and exposure of α-helix 6 may be important for membrane entry and for the modulation of RyR2 by GSTM2-2, specific residues in the C terminal domain, within α-helix 6 were mutated. Effects of these modifications on SR Ca^{2+} release and single channel experiments with lipid bilayers were evaluated.

Recombinant GST M2-2 C terminus and its mutants, F157A and Y160A were expressed and purified using the vector, pHUE. Cardiac SR vesicles were prepared from sheep heart following euthanasia by barbiturate overdose. Levels of extravesicular Ca^{2+} were monitered with antipyrylazo III, a Ca^{2+} indicator, at 710 nm using a Cary 3 spectrophotometer. Ryanodine receptor channel activity was measured using single channel lipid bilayer technique. The degree of helicity of the secondary structure of the wild type and the mutants were determined using Circular Dichroism spectroscopy.

Effects of the GSTM2-2 C terminus and its mutants, F157A and Y160A on cardiac SR Ca^{2+} release revealed that, compared to the control, all three molecules reduced the caffeine-induced Ca^{2+} release significantly ($p < 0.001$). But the inhibition produced by the mutants was significantly less ($p < 0.05$) than that produced by the wild type protein. Open probability at +40 mV was significantly reduced ($p < 0.05$) when the mutant F157A was added to the *cis* bath solution when single channel lipid bilayer experiments were conducted with cardiac SR vesicles. This mutant didn't have any voltage dependent effect on RyR2, since it showed a similar reduction in the open probability of 17.5% at -40 mV. The mutant, Y160A, when added to the *cis* bath solution produced a voltage dependent inhibition of the RyR2 with a significant open probability decrease (30%, $p < 0.05$) at +40 mV only. Similar to the results obtained for the Ca*2+* release assay, the relative open probability at +40 mV produced a significantly ($p < 0.05$) less inhibition with the mutants, F157A and Y160A, compared to the wild type GSTM2-2 C terminus. Inhibition produced by the wild type was not voltage dependent. CD spectrum revealed that the secondary structure of all three molecules has a high content of alpha helical content. In conclusion, F157A and Y160A, mutants of the GSTM2 C terminal domain have an inhibitory effect on cardiac ryanodine receptor activity but this differs from the effect of the wild type protein in magnitude (F157A and Y160A) and voltage dependence (Y160A). These differences are consistent with our hypothesis that helix 6 is important in inhibition of RyR2 and suggest that destabilizing the interaction between helix 6 and C terminal domain reduces the inhibitory action of helix 6. Since destabilization of helix 6 interactions should facilitate membrane entry, the results suggest that membrane entry is not essential for RyR2 inhibition.

Abdellatif Y, Liu D, Gallant EM, Gage PW, Board PG & Dulhunty AF. (2007) *Cell Calcium* **41:** 429–40.

Dulhunty A, Gage P, Curtis S, Chelvanayagam G & Board P. (2001) *Journal of Biological Chemistry* **276:** 3319-23.

Biophysical investigations of the cyclised skeletal muscle dihydropyridine receptor II-III loop

H-S. Tae, P.G. Board, M.G. Casarotto and A. F. Dulhunty, Division of Molecular Bioscience, The John Curtin School of Medical Research, The Australian National University, ACT 2601, Australia.

An association between the dihydropyridine receptor (DHPR) and the skeletal muscle ryanodine receptor (RyR1)is essential during skeletal muscle excitation-contraction coupling (ECC). A cytoplasmic loop connecting the 2nd and 3rd transmembrane domains (II-III loop) of the DHPR-α1s subunit has been shown to be essential for ECC (Tanabe *et al.,* 1990). A conserved RyR1-domain known as SPRY2 has been shown to bind to the DHPR II-III loop (Cui *et al.,* 2008; Leong & Maclennan, 1998). To date, *in vitro* studies on the DHPR II-III loop have been performed using the linear form of the loop (Dulhunty *et al.,* 1999). However this does not reflect the II-III loop's actual physiological state where its ends are anchored to the DHPR-α1s subunit transmembrane domains in the t-tubule membrane.

Our aim was therefore, to mimic the *in vivo* geometry of the loop using intein-mediated protein cyclisation and examine the effects. The II-III loop cyclisation was achieved through the self-catalysed ligation of the termini of the *Synechocystis sp.* PCC6803 DnaB split inteins. The results of cyclisation were determined using several techniques: i) functional-effects on native RyR1 channel activity using single channel lipid bilayer technique; ii) binding affinity to the their SPRY2 domain using fluorofluorescence spectrophotometry; and iii) secondary structural determination conducted using circular dichroism. The results of these experiments revealed that the cyclised loop produced a more pronounced effect on RyR1 channel activity, a 2-fold increase in the open probability, which was mostly due to an increase in the channel relative mean open time from 2.5 ± 0.03 ms to 8.5 ± 0.04 ms. In addition, SPRY2 domain binds to the cyclised loop 4-fold more tightly compared than to the linear loop. Circular dichroism spectroscopy suggested that the cyclised loop is considerably more α helically-structured than its intrinsically unstructured linear counterpart. This structural change could be responsible for the observed stronger effects of the cyclised loop.

In conclusion, tethering the ends of the DHPR II-III loop; to mimic its *in vivo* condition geometry resulted in: (i) a greater activator of RyR1; (ii) a tighter binding to the SPRY2 domain; and (iii) a more structured protein. This study suggests that the structure imposed on the loop by its tethering to the DHPR-transmembrane domains of could be essential in its ability to interact with RyR1 during *in vivo* ECC.

Cui Y, Tae H-S, Norris NC, Karunasekara Y, Pouliquin P, Board PG, Dulhunty AF & Casarotto MG. (2008) *International Journal of Biochemistry and Cell Biology*, **In Press**

Dulhunty AF, Laver DR, Gallant EM, Casarotto MG, Pace SM & Curtis S. 1999. *Biophysical Journal*, **77:** 189-203.

Leong P. & Maclennan DH. (1998) *Journal of Biological Chemistry*, **273:** 7791-4.

Tanabe T, Beam KG, Adams BA, Niidome T. & Numa S. (1990) *Nature*, **346:** 567-9.

Store independent activation and properties of Orai3/STIM1 mediated current

N.R. Scrimgeour and G.Y. Rychkov, Department of Physiology, University of Adelaide, Adelaide, 5005, Australia.

Recently discovered members of Orai family of proteins, Orai1, Orai2 and Orai3, form store-operated Ca^{2+} channels when expressed with stromal interaction molecule 1 (STIM1), a Ca^{2+} binding protein that plays the role of Ca^{2+} sensor in the endoplasmic reticulum. The functional properties of Orai1 have been well described using overexpression studies, but less is known about the properties of Orai2 and Orai3. The aim of these experiments was to characterise the functional properties of Orai3/STIM1 mediated current in H4IIE liver cells using whole cell patch clamping.

Overexpression of Orai3 and STIM1 generated a large store-operated Ca^{2+} current (I_{SOC}) in H4IIE cells which was activated by depletion of intracellular Ca^{2+} store by 20μM IP_3 included in the patch pipette. In general, Orai3/STIM1 mediated I_{SOC} had properties similar to that of Orai1/STIM1. Similarly to Orai1/STIM1, Orai3/STIM1 mediated I_{SOC} showed high selectivity for Ca^{2+} over monovalent cations and fast Ca^{2+} dependent inactivation at negative potentials. However, there was a significant difference between Orai1 and Orai3 in regard to the effects of 2-aminoethoxydiphenyl borate (2-APB), a known blocker of store-operated Ca^{2+} entry in a variety of cell types.

External application of 50-100μM 2-APB first briefly potentiates and then completely blocks Orai1/STIM1 mediated inward Ca^{2+} current in H4IIE cells. In contrast, we found that in cells expressing Orai3 and STIM1 50μM 2-APB caused strong rapid potentiation of the inward current, which was closely followed by rapid development of a large outward current. This effect was completely reversed by washing out of 2-APB from the bath. Analysis showed that there was a direct correlation between maximum Orai3 current amplitude and maximum 2-APB-induced inward current, indicating that 2-APB did not directly activate another type of channel. Activation of the outward current by 2-APB suggested a significant change in Orai3 selectivity. This was confirmed by cation substitutions in the external solution.

Following 2-APB application, large Orai3-mediated current existed even after removal of Ca^{2+} from the external solution, indicating that a significant part of the current was carried by Na^+. Orai3 activated by store depletion was impermeable to Cs^+ even in the absence of divalent cations. However, in the presence of 2-APB Orai3 did not discriminate between Na^+ and Cs^+, as replacing Na^+ with Cs^+ in the external solution did not affect the amplitude of the current. Oddly, we found that large cations such as $NMDG^+$ or $Tris^+$, at 10mM concentration completely blocked both inward and outward Orai3-mediated current activated by 2-APB, while they had no effect on Orai3-mediated current activated by store depletion. Voltage independence of this block suggested a more complex mechanism than a simple binding inside the pore. To investigate whether 2-APB effects on Orai3 require presence of STIM1 or depletion of the stores, we applied 2-APB to cells not transfected with STIM1 and/or without IP_3 in the patch pipette. Even without depletion of Ca^{2+} stores, no exogenous STIM1, and no development of I_{SOC}, application of 50μM 2-APB to H4IIE cells expressing Orai3 alone still activated large inward and outward currents with properties identical to those observed in cells overexpressing both Orai3 and STIM1. Therefore it appears that 2-APB activates current through Orai3 independently of Ca^{2+} stores and STIM1.

These data suggest that 2-APB increases the size of the pore formed by Orai3 polypeptides, possibly by affecting their assembly in the channel. The exact mechanism, however, remains to be investigated.

Selective and voltage dependent inhibition of N-type calcium channels by novel ω-Conotoxins CVIE and CVIF

G. Berecki,[1,2] L. Motin,[1,2] A. Haythornthwaite,[2] N.L. Daly,[3] P. Bansal,[3] S. Vink,[3] R. Drinkwater,[4] R.J. Lewis,[3,4] P.F. Alewood[3] and D.J. Adams,[1,2] [1]The Queensland Brain Institute, The University of Queensland, QLD 4072, Australia, [2]The School of Biomedical Sciences, The University of Queensland, QLD 4072, Australia, [3]The Institute for Molecular Biosciences, The University of Queensland, QLD 4072, Australia and [4]Xenome Ltd, Indooroopilly, QLD 4069, Australia.

N-type Ca^{2+} channel selective ω-conotoxins have recently emerged as potential new drugs for the treatment of severe chronic pain. In this study, two new ω-conotoxins, CVIE and CVIF, were discovered and synthesized following a PCR screen of a *Conus catus* cDNA library. All animal experimentations were performed in accordance to guidelines of the University of Queensland Animal Ethics Committee. Both ω-conotoxins potently displaced ^{125}I-GVIA binding to adult rat brain membrane. In *Xenopus* oocytes, CVIE and CVIF inhibited Ba^{2+} currents through recombinant N-type (α_{1B}, $\alpha_2\delta_1$, and β_3) channels with IC_{50} values of 2.6 ± 0.5 nM (*n* = 14) and 19.9 ± 3.2 nM (*n* = 16), respectively. Consistent with our previous study (Mould *et al.*, 2004), both peptides exhibited increased affinity for N-type Ca^{2+} channels in the absence of auxiliary $\alpha_2\delta_1$ subunit. Neither CVIE nor CVIF had any effect on P/Q-, R- or L-type calcium channels. The voltage dependence and the time course of CVIE and CVIF block were analyzed and the current recovered completely from block at -125 mV but only partially at -80 mV, indicating that CVIE and CVIF have a higher affinity to Ca^{2+} channels in the inactivated state. The analogues [R10K]CVIE and [R10K]CVIF did not significantly alter the conserved ω-conopeptide backbone conformation, but increased the rates of onset and offset of ω-conotoxin action and improved recovery from block at -80 mV, compared to the native peptides. In DRG sensory neurons isolated from neonatal rats, CVIE and CVIF potently and selectively inhibited N-type Ca^{2+} channels and the reversibility of block was voltage dependent. The R10K substitution altered the kinetics of block and was associated with an increased rate and recovery from block at -80 mV, compared to the native peptide. In rat spinal cord slices, CVIE and CVIF inhibited reversibly excitatory monosynaptic transmission between primary afferents and dorsal horn superficial lamina neurons. This result suggests the presence of an inactivation-resistant N-type Ca^{2+} channel population in the presynaptic nerve terminals. These N-type channel specific ω-conotoxins are potentially useful neurophysiological tools and inhibitors of nociceptive signaling with therapeutic implications.

Mould J, Yasuda T, Schroeder CI, Beedle AM, Doering CJ, Zamponi GW Adams DJ, Lewis RJ. (2004) *Journal of Biological Chemistry*, **279:** 34705-14.

Influence of mitochondria in the interspike interval pacemaking currents of mice *Locus Coeruleus* neurons

R.B. de Oliveira, M. Howlett, F.S. Gravina, M.S. Imtiaz, R.J. Callister, A.M. Brichta and D.F. van Helden, School of Biomedical Sciences, University of Newcastle, NSW 2308, Australia.

The *Locus Coeruleus* (LC) is a nucleus located within in the dorsorostral Pons structure of the brain stem. It comprises of noradrenergic neurons that project throughout most of the central nervous system, is the brains major source of noradrenaline and has a fundamental role in many important processes such as arousal, attention, mood and controlling behaviour. One of the features that allow LC neurons to perform their physiological functions is their synchronised rhythmical firing, providing regulated release of noradrenaline throughout the brain. Mitochondria are extremely important for neuronal function, not only for ATP production but also as an active component in calcium signalling and in the production of free radicals. Recently, neuronal mitochondria loss was linked with the promotion of some pathologies such as Parkinson's diseases (Forno, 1996; Baloyannis, 2006). Surprisingly, the death/lost of LC neurons has also been linked with Parkinson's diseases: LC neurons loose their ability to fire actions potentials and die before the classical symptoms of the diseases appear (Gesi *et al.,* 2000; Baloyannis *et al.,* 2006). As such mitochondria could be playing a role in the generation of actions potentials in LC neurons. Thus we aimed to investigate the role for mitochondria in the generation of interspike-interval pacemaker currents in mouse LC neurons. Experiments were conducted using *in vitro* brain-stem slice preparations at 37°C and whole-cell patch-clamp recordings. All procedures used were approved by the Animal Care and Ethics Committee at the University of Newcastle. To assess mitochondria participation we used three drugs, namely the protonophore CCCP, the mitochondrial Na^+/Ca^{2+} exchange inhibitor CGP-37157 and the ATPase mitochondrial inhibitor oligomycin. CCCP completely abolished the spontaneous generation of action potentials by the induction of an outward current during the interspike interval. CGP-37157 had minimum effect on the pacemaking process, slightly increasing the firing rate. Oligomycin had no effect indicating ATP depletion was not a factor. Taken together, these results indicate that mitochondria have a role in the pacemaking process. This action is seemingly mediated via the activation of an as yet unidentified outward current but does not directly involve Ca^{2+} buffering or ATP production. More studies are needed to elucidate the mitochondrial participation in the pacemaking process of mice LC neurons, and which pathways are involved.

Baloyannis SJ. (2006). *American Journal of Alzheimer's Disease*, **9:** 119-26.
Baloyannis SJ, Costa V, Baloyannis IS. (2006). *Journal of the Neurological Sciences*, **248:** 35-41.
Forno LS. (1996). *Journal of Neuropathology and Experimental Neurology*, **55:** 259-72.
Gesi M, Soldani P, Giorgi FS, Santinami A, Bonaccorsi I & Fornai F. (2000) *Neuroscience and Biobehavioral Reviews*, **24:** 655-68.

Adiponectin causes insulin secretion with increased cytoplasmic calcium and inhibition of AMP Kinase in MIN6 cells

J.R. Rao,[1,2] H.C. Parkington,[2] D.J. Keating[1] and C. Chen,[1,2] [1]Prince Henry's Institute of Medical Research, Clayton, VIC 3168, Australia and [2]Department of Physiology, Monash University, VIC 3800, Australia.

Type 2 diabetes is a growing concern and, according to World Health Organisation (WHO) figures, is poised to increase by 114% in the next 20 years. It is characterised by an initial reduction in glucose uptake by skeletal muscle and adipose tissue due to insulin resistance. This is compounded, later in the disease, by a reduction in insulin secretion by pancreatic β cells in response to increasing blood glucose. Type 2 diabetes is tightly linked to obesity, an increase in adipose tissue. Adipose tissue is an active endocrine organ, secreting many adipokines with important physiological actions. Adiponectin is a recently discovered adipokine whose levels, paradoxically, are decreased in obesity despite the increase in adipocyte mass (Pajvani & Scherer, 2003). Adiponectin suppresses triglyceride accumulation, increases fatty acid oxidation and activates AMP kinase (AMPK) in skeletal muscle, improving insulin signalling. Adiponectin also suppresses glucose production and activates AMPK in liver. Hence, adiponectin is an insulin sensitizer in skeletal muscle (Berg *et al.*, 2001; Yamauchi *et al.*, 2003). Adiponectin receptors have been reported in pancreatic β cells (Kharroubi *et al.*, 2003). AMPK indicates cellular energy status and has been implicated in the process of insulin secretion. Elegant studies in clonal β cell lines and primary islets demonstrate that increasing glucose concentration inhibits AMPK activity, accompanied by enhanced insulin secretion (da Silva Xavier *et al.*, 2003).

We hypothesised that adiponectin modifies insulin secretion and AMPK activity via its receptors on pancreatic β cells. We investigated the effects of adiponectin on pancreatic β-cell function by assaying insulin secretion using ELISA, quantifying AMPK phosphorylation using western blotting and imaging intracellular free calcium concentration ($[Ca^{2+}]_i$,), using the Ca^{2+} sensitive flurophore, Fluo-3, using MIN6 cells, a murine pancreatic β-cell line. We investigated the effect of adiponectin on AMPK and insulin secretion using AICAR, a known AMPK activator, and KN-62 an inhibitor of this enzyme.

Adiponectin (2μg/ml) suppressed AMPK activity and caused an increase in insulin secretion. Acute (30min) application of adiponectin caused a prompt increase in $[Ca^{2+}]_i$ (Figure). The increases in $[Ca^{2+}]_i$ and insulin production were prevented by nifedipine, a blocker of L-type Ca^{2+} channels, and did not occur in Ca^{2+} free solution. The suppression of AMPK activity and increases in insulin and $[Ca^{2+}]_i$ induced by adiponectin were comparable to those evoked by a physiological high glucose stimulation (Table). The effect of adiponectin on insulin secretion was potentiated in the presence of AICAR and KN-62.

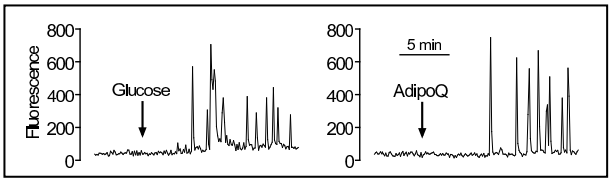

	pAMPK/tAPMK	Insulin	$[Ca^{2+}]_i$
Adiponectin (3mM glucose)	48±10% (*p*=0.01)	303±51% (p=0.001)	142±14% (*p*=0.03)
25mM glucose	68±6% (*p*=0.01)	173±12% (*p*=0.001)	161±11% (*p*=0.01)

In conclusion, we show that the fat hormone adiponectin is capable of increasing pancreatic β cell Ca^{2+}, giving rise to insulin secretion. Adiponectin also suppresses phosphorylation of AMPK to augment insulin production. The decrease in adiponectin in obesity likely impairs this system. These results reveal the potential of adiponectin as a novel therapeutic target against obesity-linked type 2 diabetes.

Berg AH, Combs TP, Du X, Brownlee M, Scherer PE. (2001) *Nature Medicine*, **7**, 947-53.

da Silva Xavier G, Leclerc I, Varadi A, Tsuboi T, Moule SK, Rutter GA. (2003) *Biochemistry Journal*, **371**, 761-74.

Kharroubi I, Rasschaert J, Eizirik DL, Cnop M. (2003) *Biochemical and Biophysical Research Communications*, **312**, 1118-22.

Pajvani UB, Scherer, PE (2003) *Current Diabetes Reports*, **3**, 207-13.

Yamauchi T, Kamon J, Ito Y, Tsuchida A, Yokomizo T, Kita S, Sugiyama T, Miyagishi M, Hara K, Tsunoda M, Murakami K, Ohteki T, Uchida S, Takekawa S, Waki H, Tsuno NH, Shibata Y, Terauchi Y, Froguel P, Tobe K, Koyasu S, Taira K, Kitamura T, Shimizu T, Nagai R, Kadowaki T. (2003) *Nature*, **423**, 762-9.